Knock-out of Flotillins in Human Cells Using the CRISPR-Cas9 Genome Editing System: Effects on mRNA Splicing

Inaugural Dissertation
Submitted to the Faculty of Medicine
for Partial Fulfilment of the Doctoral Degree in Medicine at
Justus-Liebig-University Gießen

Submitted by

Marcel Kapahnke

Born in Bad Homburg v.d.H., Germany

Gießen 2020

From the Institute of Biochemistry
Faculty of Medicine
Justus-Liebig-University Gießen
Director of the institute: Prof. Dr. Lienhard Schmitz

Supervisor: Prof. Dr. Ritva Tikkanen
Supervisor: Prof. Dr. Saverio Bellusci

Date of doctoral defence: 28/10/2020

Table of Contents

I. Introduction

I.1 Flotillins

I.1.1 Discovery

The two homologous flotillin proteins were discovered in 1997 by two independent working groups. Schulte et al. found out that flotillins are involved in neuronal regeneration processes in goldfish. Due to this function, they called the newly found proteins “reggies” (Schulte et al. 1997). Another group, around Bickel et al., performed cell culture studies with different types of murine tissues and spotted flotillins in caveolae (Bickel et al. 1997). The name “flotillin” derives from the insoluble characteristics of caveolar domains in Triton X-100 and the resulting floating characteristics. Nowadays the term flotillin has become the more common name for this protein family. Because of their independent discovery, reggie-1 is equivalent to flotillin-2 and reggie-2 to flotillin-1.
Even prior to these discoveries, in 1994, the existence of flotillin-2 was described in human skin and the protein was called Epidermal Surface Antigen (ESA) (Schroeder et al. 1994). This protein was thought to be involved in cell adhesion and maintenance in human skin and later was discovered to be identical with flotillin-2.

I.1.2 Localisation

The initially assumed localisation of flotillins exclusively in caveolae, as suggested by Bickel et al., turned out as not valid (Bickel et al. 1997). Flotillins have now been spotted in cell types such as neurons and lymphocytes that lack caveolin, the structural protein for caveolae, and are thus incapable of forming caveolae (Stuermer et al. 2001).
Flotillins are located in membrane rafts (Figure I-1a). These are membrane microdomains enriched in cholesterol and glycosphingolipids. Lipid rafts are assumed to be involved in various pathways such as T-cell receptor (TCR) signalling, HIV assembly, endoplasmic reticulum and Golgi trafficking, as well as glycosphingolipid-mediated endocytosis (Simons and Gerl 2010). Nowadays, flotillins are well established as marker proteins for certain kinds of membrane rafts (Banning et al. 2014).

The localisation of flotillins can be variable. It depends on the cell type and differentiation status and can be changed by stimulants such as EGF. In HeLa cells, which were used in this study, flotillins reside mainly at the plasma membrane. Other localisation sites are endosomes, lysosomes, exosomes (flotillin-1), the Golgi (flotillin-1) and the nucleus (flotillin-1) (Banning et al. 2014).

I.1.3 Structure

Even though their genes reside on two different chromosomes (*FLOT1* on chromosome 6, *FLOT2* on chromosome 17), flotillins exhibit a high similarity (50% identity on mRNA level and 44% on protein level). The identity of the amino acid sequence in different mammalian organisms is very high. The human and murine flotillin-1 coincide in 98.1% of their amino acid sequence. Both flotillins have a molecular weight of approximately 47 kDa (Banning et al. 2014).

Right from the beginning of their discovery, flotillins were predicted to be associated with the plasma membrane, even though they do not contain any transmembrane domains. Contact with hydrophobic membranes is mediated by fatty acid modifications and hydrophobic amino acid sequences in the N-terminal part (Morrow and Parton 2005). The localisation of the modification sites and the identity of the fatty acids differ in both flotillins. Flotillin-1 is palmitoylated only at Cys34, which is needed for the membrane association in kidney cells (Morrow et al. 2002). Another group around Liu et al. found out that two hydrophobic domains are responsible for the localisation at membranes in adipocytes. These data suggest that the localisation of flotillin-1 is cell type dependent and mediated by different structures (Liu et al. 2005). Membrane attachment of flotillin-2 is accomplished in a different manner. Myristoylation at Gly2 and three palmitoylation sites at cysteines Cys4, Cys19 and Cys20 mediate the membrane association of flotillin-2. The myristoylation at Gly2 was proven to be a prerequisite for any further acylation (Neumann-Giesen et al. 2004) (Figure I-1b).

Both flotillins have a stomatin, prohibitin, flotillin and HflC and K (SPFH) domain, also known as the prohibitin homology (PHB) domain, localised in their N-terminus. The exact function of this domain has not been identified by now, but most proteins containing such SPFH domains are associated with membrane rafts and have the capacity to form oligomers

(Browman et al. 2007). In addition to other members of the SPFH protein family, flotillins exhibit a highly conserved C-terminus, the so-called flotillin domain. This domain is responsible for the oligomerisation (Solis et al. 2007).

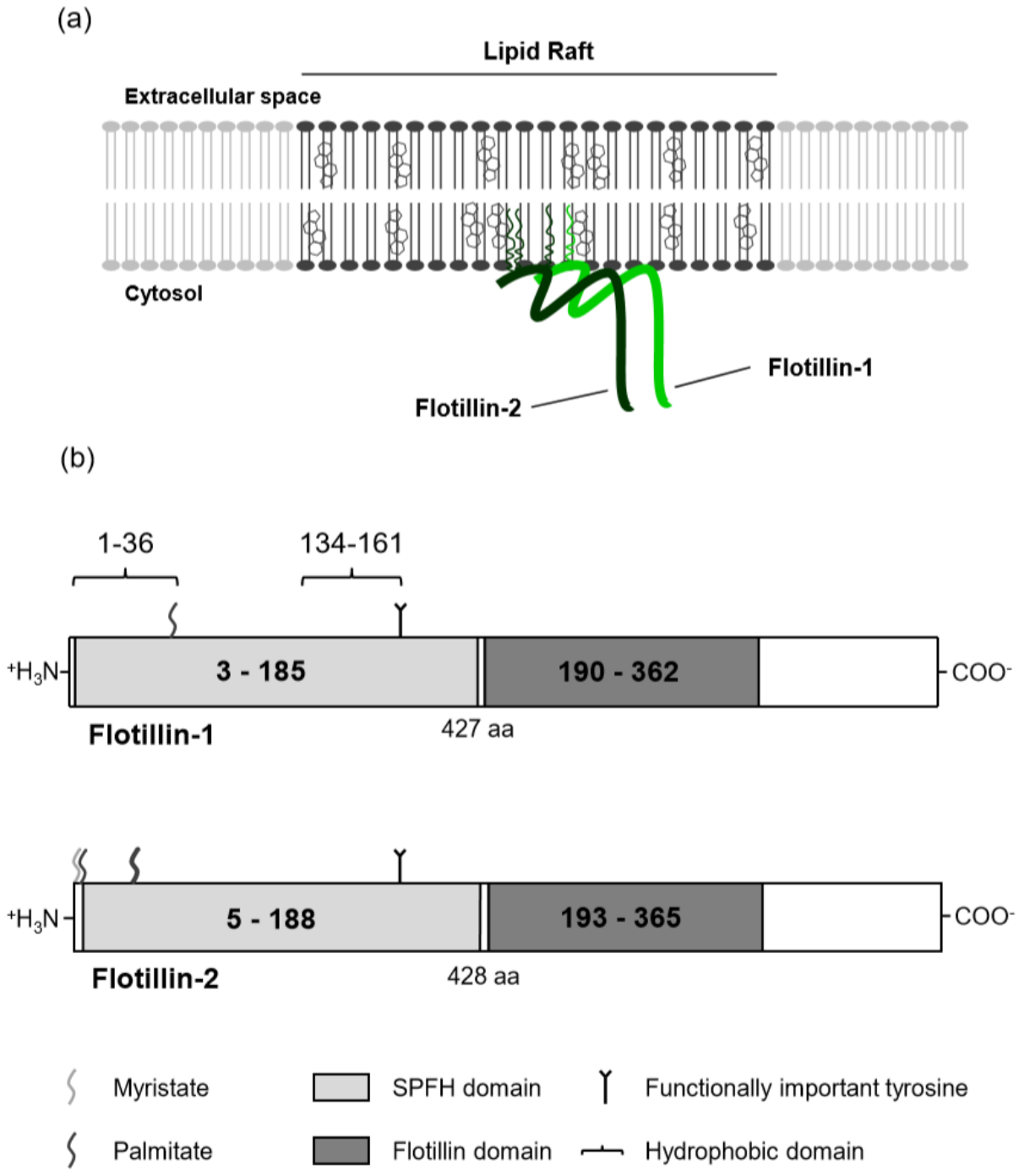

Figure I-1: (a) Membrane rafts are cholesterol and glycosphingolipid enriched microdomains in the plasma membrane. Flotillins associate with rafts via fatty acid modifications and hydrophobic amino acid sequences

and form hetero- or homooligomers. **(b)** Domain structure of flotillins. Human flotillin proteins are 44% identical with each other and have an N-terminal SPFH domain and a C-terminal flotillin domain. In flotillin-1, there are two hydrophobic domains mediating membrane association. (Figure adapted from Meister 2014)

I.1.4 Function

Flotillins have been shown to be involved in a number of cellular processes. Their functions seem to depend on the tissue type as well as the expression pattern and the cellular localisation. One of their functions has been suggested to be associated with an endocytosis pathway independent of clathrin and dynamin (CIE) (Frick et al. 2007; Glebov et al. 2006). Later studies assumed that flotillins are also involved in the classical clathrin-dependent endocytosis (Sorkina et al. 2013). The exact role of flotillins in cellular trafficking pathways is still not fully understood, but numerous examples for their participation in cargo processing have been found (Meister and Tikkanen 2014). Later studies have shown that flotillins play a role in exocytosis and endosomal sorting of the β-site amyloid precursor protein-cleaving enzyme 1 (BACE1) (John et al. 2014).

Another role of flotillins has been suggested to lie within the insulin receptor signalling. The main signal transduction after stimulation with insulin is mediated by Phosphoinositide-3-Kinase (PI3K). An alternative, more fine-tuning pathway involves the interaction of Cbl-associated protein (CAP) and Casitas B-lineage Lymphoma (c-Cbl) which are phosphorylated and form a complex. The recruitment of this effector complex to membrane rafts requires the presence of flotillin-1 (Baumann et al. 2000).

Cell adhesion is mediated by desmosomes, and many desmosomal proteins are located in membrane rafts. Hence, also flotillins that are located in this microdomain are involved in the dynamics of this adhesion structure (Resnik et al. 2011). Furthermore, flotillins have been shown to interact with γ-catenin, which is present in adherens junctions as well as in desmosomes (Kurrle et al. 2013). Völlner et al. could also show a colocalisation of flotillins and desmoglein-3 and weakened desmosomal adhesion in flotillin depleted human keratinocytes (Völlner et al. 2016).

I.1.5 Flotillins in growth factor signaling and apoptosis

An important function of flotillins is within growth factor signalling and the subsequent mitogen activated protein kinase (MAPK) activation. On the one hand both flotillins are upregulated in many cancer cells, indicating that they might support cancer growth and be a possible target for future cancer therapies. On the other hand, different findings show that also the absence of flotillins may lead to an increased activity of mitogenic pathways (Banning et al. 2014).

Most growth factor receptors, such as the epidermal growth factor receptor (EGFR), are tyrosine kinases. Stimulation with the respective ligand results in receptor dimerisation and autophosphorylation of tyrosine residues. The activated receptor recruits diverse signalling molecules, which leads to a kinase-mediated signal cascade beginning with the Ser/Thr kinase RAF (rapidly accelerating fibrosarcoma). The activated RAF protein phosphorylates and thus activates the MAPK/ERK Kinase (MEK) which, as the name indicates, is responsible for the phosphorylation of the extracellular signal regulated kinase (ERK). ERK has more than 200 substrates that, upon phosphorylation by ERK, support cell growth and mitosis. Although flotillin expression is ubiquitous, their gene expression can be regulated by two substrates of ERK, the transcription factors early growth response protein 1 (Egr1) and serum response factor (SRF) (Banning et al. 2012).

After EGF stimulation, flotillins are target proteins in the subsequent signal cascade and go through several changes concerning oligomerisation, phosphorylation and the distribution pattern. Stimulation with EGF results in an increase in the size of flotillin oligomers (Babuke et al. 2009), and flotillin-2 gets phosphorylated by Src kinases at several Tyr residues (Neumann-Giesen et al. 2007). Also the subcellular localisation of flotillins is changed after EGF stimulation, since flotillins are endocytosed from the cell membrane into late endosomes (Neumann-Giesen et al. 2007). It has been shown that Y160 in flotillin-1 and Y163 in flotillin-2 are a prerequisite for endocytosis, but their phosphorylation by Src kinases is not the driving force. More important for the endocytosis seems to be a hetero-oligomerisation of both flotillins, since flotillin-1 knock-down cells are not able to endocytose flotillin-2 (Babuke et al. 2009).

Other experiments with flotillin-1 knock-down HeLa cells showed that the phosphorylation of EGFR and ERK upon stimulation with EGF is decreased (Amaddii et al. 2012). These data imply that flotillin-1 is a scaffolding factor in the early phase (activation of the receptor) and in a late phase (activation of the MAP kinase pathway) of growth factor signalling (Amaddii et al. 2012). In contrast to that, flotillin-2 knock-down has opposite effects on MAP kinase signalling. In flotillin-2 knock-down HeLa cells, ERK activation upon EGF stimulation is increased (Banning et al. 2014). Based on these data, a possible targeted therapy against flotillins needs to be regarded critically, as ablation of flotillin-2 may increase growth-promoting signalling in cancer cells (Banning et al. 2014).

Interestingly, a mitogenic effect was reported also upon flotillin-1 ablation. Kurrle et al. discovered an increased level of EGFR and hyperactivation of MAPK signalling in flotillin-1 knock-down MCF7 breast cancer cells (Kurrle et al. 2013). To elucidate the exact role of flotillin-1 and -2 in receptor tyrosine kinase signalling, more research is required. Thus, at the moment there is not enough detailed knowledge about the impact of flotillins on cancer cell signalling to seriously consider cancer therapies targeting flotillins.

Apoptosis is the pathway for programmed cell death, which can be provoked by an intrinsic or an extrinsic pathway. The balance of pro- and anti-apoptotic signals determines whether a cell undergoes apoptosis or not. Flotillins have been shown to contribute to the maintenance of the balance of survival and apoptotic signals (John 2014). Many cancer cells show an impaired balance of these signals having a reduced rate of apoptosis. The role of flotillins in apoptosis pathways was analysed by John in her PhD thesis: The absence of flotillins leads to a reduction of anti-apoptotic signals upon treatment with staurosporin (STS), indicating that flotillins support to cell survival (John 2014).

I.2 Genome editing systems

Genome editing systems are nowadays integral parts in biomedical science. Their aim is to modify DNA sequences in a specific manner. Therefore, their design typically consists of a nuclease, which is guided by a DNA-binding unit towards its specific target. A major challenge is always to provoke a unique DNA modification without any off-target effects, which still remains an enormous issue in research based on these methods.

Zinc finger nucleases (ZFNs) were the first application of specific double strand break inducing systems. ZFNs do not occur naturally, but they are composed synthetically of two subunits. Their DNA-binding subunit is a zinc finger domain, whose nomination originates from the fact that they bind a zinc ion between an α-helix and an antiparallel β-sheet, making them look like a finger. The first six amino acids of a zinc finger are able to recognise a specific base triplet on the DNA through binding at the major groove. Rows of three or four of these domains are put together to a zinc finger protein to increase the binding specificity. The DNA-binding part is coupled with the nuclease FokI, a restriction enzyme derived from Flavobacterium okeanokoites. The target of a ZFN can be adjusted by modifying the base triplet specificity of a single zinc finger or by changing the arrangement of different zinc fingers within the zinc finger domain (Kim et al. 1996).

Transcription activator-like effector nucleases (TALENs) are another method for genome editing. As the ZFN, they are synthetic proteins and consist of the nuclease FokI and a DNA-binding part. TAL (transcription activator-like) effectors, the DNA-binding subunits, originate from the phytopathogenic bacteria Xanthomonas. In contrast to zinc finger domains, TAL effectors spot one single base and not a base triplet. TAL effectors have a conserved amino acid sequence of 33 and 34 residues. Only residue 12 and 13, the so called repeat variable di-residue (RVD), is variable, being responsible for the specific recognition of one of the four nucleobases. For experiments aiming at targeting a specific site in the DNA, 12 – 15 RVDs are coupled with FokI (Ding et al. 2013).

RNA interference (RNAi) is a posttranscriptional regulation pathway that causes a degradation of a specific messenger RNA (mRNA). This process occurs *in vivo* but may be manipulated for scientific research. Using this method, it is not possible to achieve a complete absence of the targeted protein; but an effective downregulation of the respective gene product is typically observed, and thus called knock-down to differentiate it from the complete gene knock-out. Originally, RNA interference is a natural cellular regulation mechanism for protein expression, but it is also in charge of immune defence against viruses. In science, this mechanism can be exploited for specific downregulation of protein expression level. The formation of a complementary dsRNA, called short interfering RNA (siRNA), to the targeted mRNA stands at the beginning of every RNAi. The Endonuclease argonaute 2 (AGO2) forms the RNA-induced silencing complex (RISC) together with the

siRNA. In the RISC, only the antisense strand remains, whereas the sense strand gets degraded. By hybridising with the target mRNA, the single antisense strand of the siRNA leads AGO2 towards its target.

The dsRNA at the beginning can be produced either by the cell itself or it can be delivered by transfection. It is possible to achieve either a transient knock-down using siRNAs or a stable knock-down using a precursor shRNA (short hairpin RNA), whose DNA copy is integrated into the genome of the target cell, where it is continuously transcribed into the specific shRNA (Rana 2007).

I.3 CRISPR-Cas9 genome editing system

I.3.1 Bacterial origin

The CRISPR-Cas9 system (Clustered regulatory short palindromic repeats) is part of the bacterial immune system with the task of eliminating foreign DNA originating from viruses or plasmids (Makarova et al. 2011). It contains the nuclease Cas9 (CRISPR associated) and the two RNA particles crRNA (CRISPR-RNA) and tracrRNA (trans-activating-CRISPR-RNA). The CRISPR locus contains several DNA sequences called repeats and 20 base pair long spacers. Every spacer has its origin in different types of invading plasmids or viral DNA, while all the repeats have the common characteristic DNA sequence and separate the spacers form each other (see Figure I-2). The transcript of this locus is called pre-crRNA. To become a mature CRISPR-Cas9 complex, the tracrRNA binds to the repeats and mediates the binding of Cas9. Cleavage into smaller RNA units of 1 repeat and 1 spacer, called crRNA, is performed by the endogenous RNase III (Mali et al. 2013).

Since every spacer sequence derives from a different viral DNA segment or plasmid, it is able to detect the corresponding complementary DNA of its origin via Watson-Crick base pairs. If a protospacer adjacent motif (PAM) immediately precedes the homologous target strand, a double strand break will be produced in the target DNA by the nuclease Cas9. The CRISPR-Cas9 system traditionally used in scientific studies was derived from Streptococcus pyogenes and requires a 5′-NGG PAM following the 20 bp long spacer motif. PAMs are missing in the genomic CRISPR region to protect the bacterial DNA from cleaving itself (Horvath and Barrangou 2010).

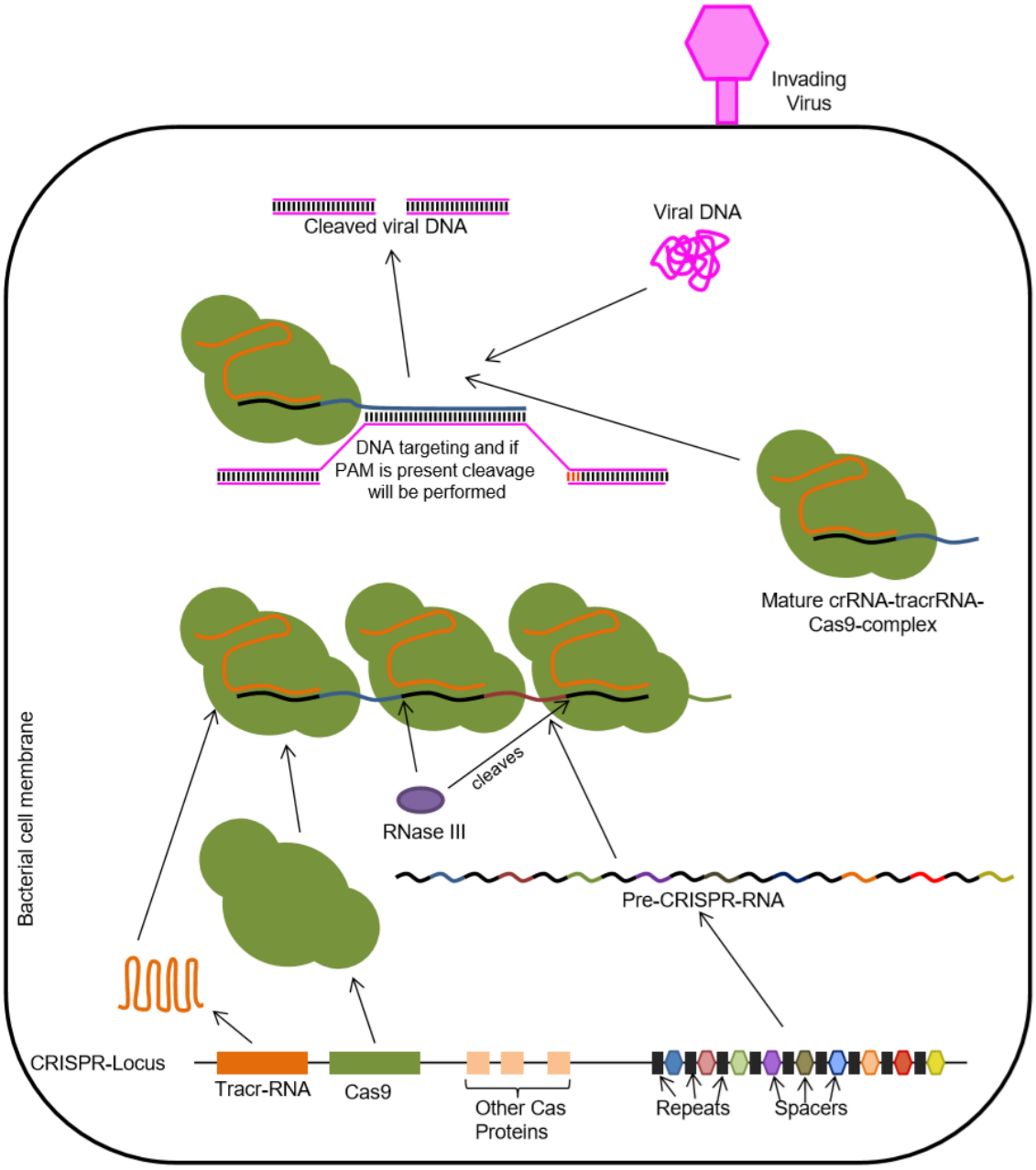

Figure I-2: The CRISPR locus is the area on bacterial DNA where the information for tracrRNA, CRISPR-RNA and the nuclease Cas9 is located. The pre-CRISPR-RNA originates from a DNA area consisting of short repeats, which have a conserved sequence, alternating with spacers, which originate from former invading DNA and have a target specific sequence. To form the CRISPR-Cas9 complex, the tracrRNA joins to the RNA pre-transcript via complementary binding to the repeats. The nuclease Cas9 can now bind to the complex of pre-CRISPR-RNA and tracrRNA. The long string of one pre-CRISPR-RNA, tracrRNAs and Cas9 nucleases gets divided into smaller units by the bacterial RNase III. Now the mature crRNA-tracrRNA-Cas9-complex can be directed towards the specific DNA sequence of the spacers' origin. As the spacer originates from a foreign DNA particle such as viral DNA, it is able to bind homologous to the complementary strand of its origin. If a protospacer adjacent motif (PAM) immediately precedes the target sequence, a double-strand break gets introduced on the invading DNA. The PAM is not present on the bacterial genome to protect it from autocleavage. (Figure adapted from Mali et al. 2013, changes in colouring, design and absence of some details without significance for this project)

I.3.2 Application in scientific studies

For scientific purposes, CRISPR-Cas9 is a method of interest, because Cas9 complex can be directed to almost any target of interest located next to a PAM by simply modifying the 20 bp long spacer sequence. This sequence can be cloned into a plasmid that includes the information for Cas9, and the resulting plasmid can be transfected into human cells (Ran et al. 2013).

The application in eukaryotic cells brings some new challenges. The transcripts synthesised by the eukaryotic RNA-polymerase II receive a 5'-guanosyl-cap and 3'-poly-A tail and are translocated into cytosol. The crRNA and tracrRNA form a secondary structure, which would be degraded by the endoribonuclease Dicer if it was an mRNA. Hence, it is necessary to design plasmids with a promoter for the RNA-polymerase III (RNAP III), whose transcripts are not processed and remain in the nucleus. The promotor U6 is one of the few RNAP III promotors whose transcription factor binding sites are localised upstream of the transcribed sequence and not within it. To improve hybridisation of crRNA and tracrRNA, their DNA sequences are merged to form a chimeric, common transcript called single guide RNA (sgRNA) (Ran et al. 2013). Furthermore, Cas9 has to be modified by means of a nuclear localisation sequence (NLS) for translocation backwards into nucleus after the cytosolic translation.

Finally, Cas9 and sgRNA form a ribonucleoprotein that can induce double strand breaks (DSB) at target sites with a homologous sequence to the sgRNA. The defect caused by the DSBs is repaired via non-homologous end joining (NHEJ). Due to this error-prone mechanism, small insertions or deletions, called indel mutations, are introduced at the DNA target side. If such an indel mutation is not a multiple of 3, the resulting frameshift is supposed to cause a stop codon a few triplets downstream, so that the information for a functional protein is deleted (Mali et al. 2013).

I.3.3 Recent development of CRISPR-Cas9

The experiments for this study have been performed in 2015, when CRISPR-Cas9 was a rather new approach. Since then, CRISPR-Cas9 has become the most meaningful genome editing tool and is widely used (Wang et al. 2019). Despite the short period of time from its

discovery until now, but with regards to its extensive use, huge efforts have been taken to improve its function and precision.

Even though gRNAs are designed carefully and the DNA-binding sequence is predicted to be unique in the genome of the target organism, the DNA binding is not always 100% specific. The use of CRISPR-Cas9 is thus prone to cause off-target double strand breaks. Therefore, great caution is needed especially when modifying stem cell populations in real patients (Vakulskas et al. 2018). Many tools are now available to identify potential off-target DNA cleavage sites, and the likely hits should be verified after the modification with CRISPR-Cas9, in order to exclude such off-target effects (Hu et al. 2016).

One new approach in the CRISPR-Cas9 technology is a novel delivery method into the cell. Whereas earlier, hence also in this study, the gRNA and the *cas9* gene were cloned into a plasmid, and this plasmid was transfected into the host cell, newer techniques focus on the formation of a ribonucleoprotein (RNP) complex prior to cellular delivery (Jacobi et al. 2017). This RNP can be transfected directly via lipofection or electroporation into the host cell. Overexpression and thus unspecific binding of gRNAs may lead to DNA cleavage at off-target sites when using plasmid templates for the CRISPR-Cas9 complex (Fu et al. 2013). By means of a directly introduced and competent gRNA/Cas9-complex, the concentration of the genome editing machinery does not depend on the protein expression in the target cell and can thus be more easily fine-tuned.

Another improvement has been the discovery of diverse Cas9 mutants with less off-target effects but high on-target efficiency (Vakulskas et al. 2018). One mutant, called high-fidelity (HiFi) Cas9, is predicted to have wide utility in basic science and to be even qualified for therapeutic issues because of its high specificity. In fact, a phase I clinical study for sickle cell disease using new Cas9 mutants and RNP delivery has already started (Vakulskas and Behlke 2019).

I.4 Splicing

I.4.1 Operating principal

Most bacterial proteins are encoded by only one continuous chain of nucleic acid triplets. In contrast to that, most genes in higher eukaryotic organisms are interrupted by intragenic non-coding sequences, called introns. The protein-expressing regions, together with the two untranslated regions (UTR) of the mRNA, are called exons. As a consequence, the RNA product directly after transcription by means of the RNA polymerase II, the so called precursor mRNA (pre-mRNA), needs to be processed by excising all introns (Newman 1998). This process, called splicing, needs to be carried out with a high accuracy, since errors in the number of excised bases are likely to cause a frameshift. Nearly every intron begins with a GU sequence and ends with an AG preceded by a pyrimidine enriched section (see Figure I-3).

Splicing is carried out by spliceosomes, which are large ribonucleoprotein complexes built up stepwise around a pre-mRNA. This complex consists of five spliceosomal small nuclear ribonucleoprotein particles (snRNPs) U1, U2, U4, U5 and U6 and numerous other proteins, so that the size of a spliceosome can be compared to the ribosome complex (Brody and Abelson 1985). Chemically, splicing comprises two trans-esterifications, which per se are energetically neutral, but rearrangement of the snRNAs requires several ATP-dependent steps. The reaction begins with a 2'-OH-residue of an adenylate, located in the pyrimidine-enriched section, attacking the 5'-phosphate end of the intron, forming a 2'-5'-phosphodiester bond. The resulting free 3'-OH residue of the upstreaming exon end can now attack the downstream 5'-phosphate residue of the next exon, with the two exons joining together and excising the intron sequence in a lariat form (Staley and Guthrie 1998). For a long time, excised introns have been considered as junk ready for degradation, but recent studies have discovered further functions of introns as small nucleolar RNAs, microRNAs, long non-coding RNAs or regulators of translation and virus latency (Hesselberth 2013).

In some genes, there are different possibilities for splicing, which enables the generation of diverse protein products from the same DNA region. This capacity is called alternative

splicing and is possible due to an excision of selected exons as if they were introns (Cáceres and Kornblihtt 2002). This mechanism has e.g. been observed in antibodies but has never been described for flotillins.

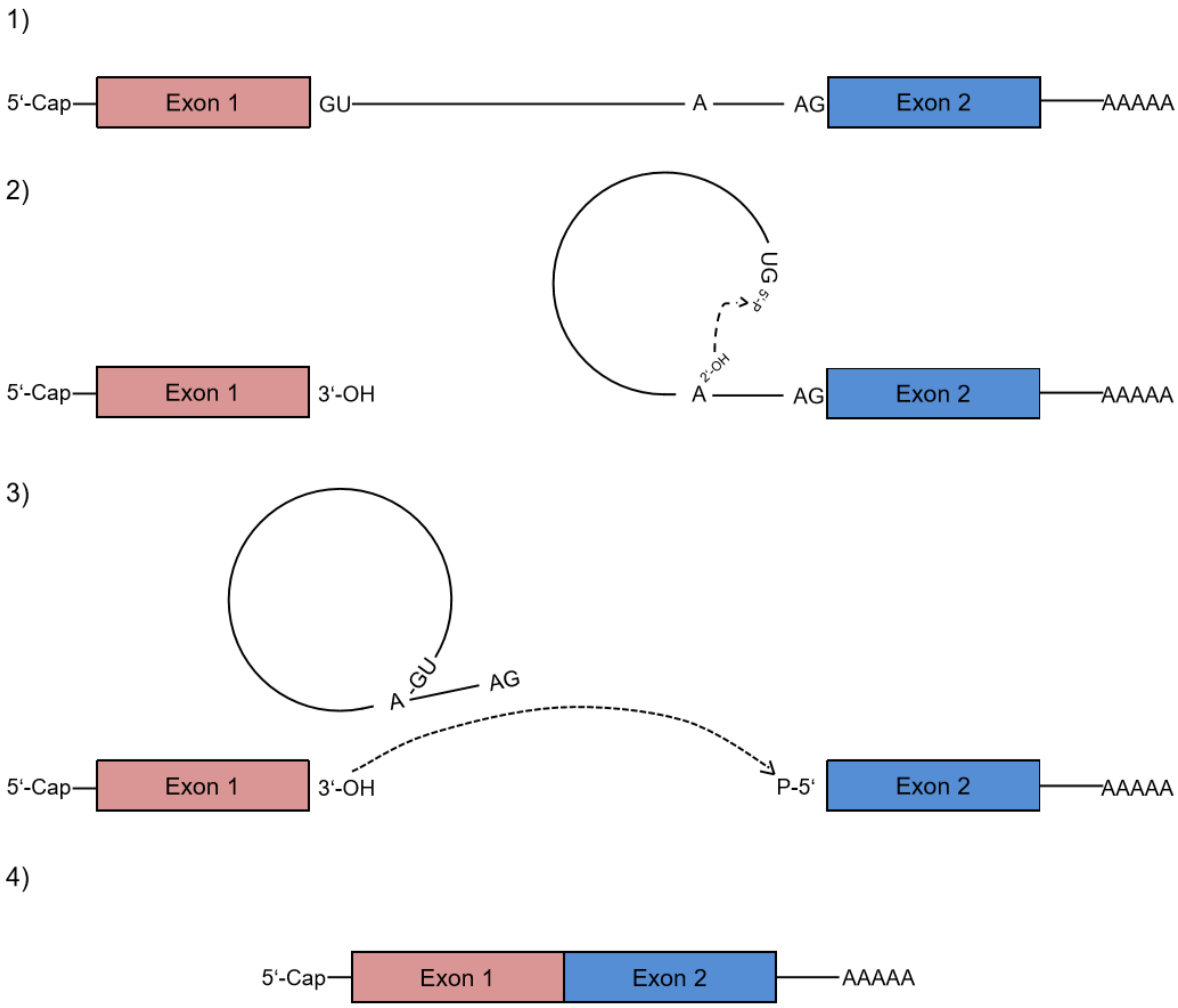

Figure I-3: Scheme of the splicing mechanism. Most introns are margined by GU and AG sequences. An A residue within the intron is also of importance, as the first step is an attack of the 2'-OH group of this A on the 5'-phosphate group of the G at the beginning of the intron, forming a phosphodiester bond. The resulting free 3'-OH group of the preceding exon can now attack the 5'-phosphate group of the downstream exon, merging together and excising the intron in a lariat form. This process and its high precision are mediated by several subunits of the spliceosome, which is not depicted in this figure.

I.4.2 Alteration of splicing

Little is known about how the factors involved in splicing are able to fulfil the high demands on their function. The correct recognition of diverse splicing sites, precise excision of introns and the regulation of alternative splicing need to be carried out with high fidelity in order to produce a correct protein sequence (Baralle and Buratti 2017). The recognition sites GU and AG preceded by a pyrimidine enriched section alone do not seem specific enough for a precise recognition site, as they consist only of two bases. However, splicing elements can be guided by diverse intronic (ISE) and exonic splicing enhancer (ESE) or suppressor (ESS and ISS) towards the correct splicing sites (Wang and Cooper 2007).

Studies of the last two decades have described several factors that influence the fidelity of the splicing machinery. These factors are point mutations in the exon regions (Vockley et al. 2000), chromatin conformation in co-translational splicing (Iannone and Valcárcel 2013), ncRNA-binding sites (Khanna and Stamm 2010), secondary structure of the pre-mRNA (Buratti and Baralle 2004), extracellular signalling pathways (Shin and Manley 2004), and several drugs (Zaharieva et al. 2012). Furthermore, various bioinformatic programs have emerged in order to predict splice sites (e.g. Automated Splice Site Analyses or Human Splicing Finder) (Baralle and Buratti 2017). Although many efforts have been undertaken to illuminate the complex role of the splicing machinery, it is not yet possible to predict the impact of changes on the involved actors mentioned above.

Defects of splicing have been shown to occur in approximately 15–50% of all human disease mutations, which gives splicing a crucial role not only in monogenic hereditary diseases, but also in more complex disorders like cancer and degenerative diseases (Baralle and Buratti 2017).

I.5 Aims of the present study

Cells with knock-down due to RNA interference still have a reduced level of the target protein, which might be enough for a persisting protein function. Most experiments with flotillins have been performed using such knock-down cell lines. Thus, the aim of this study was to create flotillin knock-out cell lines using the CRISPR-Cas9 system, which show a complete absence of either one or both flotillins. CRISPR-Cas9 is supposed to be a more precise and less work-intensive tool for genome editing than other similar methods. The associated workload is far less as compared to TALENs and ZFNs, since only a single gRNA is sufficient for the specific gene targeting. The new cell lines generated here were analysed on protein, mRNA, and genomic DNA level. The results in the created flotillin knock-out cell lines were compared to the previously generated flotillin knock-down cell lines.

II. Materials and methods

II.1 Chemicals and technical devices

II.1.1 Technical devices

Table II-1: Technical devices.

Device	Manufacturer	Model
Accuracy weighing machine	Sartorius, Göttingen, Germany	SI-64
Bacteria shaker	Edmund Bühler, Tübingen, Germany	TH 15
Camera	Canon, Tokio, Japan	Powershot A470
Centrifuges	Hettich, Tuttlingen, Germany	Mikro 22R
	Hettich, Tuttlingen, Germany	Mikro 200R
	Hettich, Tuttlingen, Germany	Universal 32R
	Hettich, Tuttlingen, Germany	Universal 320
	Labnet International, Edison, NJ, USA	C 1301B
	Eppendorf, Hamburg, Germany	miniSpin plus
	Beckman Coulter, Brea, CA, USA	J2-21
Clean bench	Thermo Scientific, Waltham, MA, USA	Herasafe KS
Developing machine	AGFA, Mortsel, Belgium	Curix 60
Incubator for bacteria	MMM, Munich, Germany	Incucell
Incubator for eukaryotic cells	Sanyo, Moriguchi, Japan	CO2 incubator MCO-2OAIC
Electrophoresis chambers	Amersham Biosciences, GE Healthcare, Chalfont St Giles, UK	Mighty Small II
	neoLab, Heidelberg, Germany	Midi Large

Heating blocks	HLC, Bovenden, Germany	HBT-2 131
	HLC, Bovenden, Germany	HTME 131
Microscope	Motic, Xiamen, China	AE31
	Zeiss, Oberkochen, Germany	LSM 710
Nanodrop plate	Tecan, Männedorf, Switzerland	NanoQuant plate™
PCR thermocycler	Biometra, Göttingen, Germany	T personal
Photometer	Eppendorf, Hamburg, Germany	BioPhotometer plus
Power supply	Amersham Biosciences, GE Healthcare, Chalfont St Giles, UK	EPS-301
Plate reader	Tecan, Männedorf, Switzerland	Infinite M200
Rotating wheel	neoLab, Heidelberg, Germany	Rotator 2-1175
Shaking devices	Edmund Bühler, Tübingen, Germany	WS 10
	Heidolph Instruments, Schwabach, Germany	Polymax 1040
Sonicator	Bandelin, Berlin, Germany	Sonopuls
UV transilluminator	Konrad Benda Laborgeräte, Wiesloch, Germany	NU-72 MI
Vortex mixer	Peqlab biotechnologie, Erlangen, Germany	Bio-Vortex V1
Water bath	Fried Electric, Haifa, Israel	WBS-11
Water purification system	Merck Millipore, Darmstadt, Germany	Elix
Weighing machine	Mettler Toledo, Greifensee, Switzerland	PB602-S
Western blot chamber	Bio-Rad Laboratories, Hercules, CA, USA	Criterion Blotter
qPCR machine	Applied Biosystems, Thermo Fisher Scientific GmbH, Dreieich, Germany	PCR System 2700, Gene Amp

Consumables, e.g., reaction tubes, pipette tips, falcons, cell culture flasks and plates were purchased from BD Biosciences (Franklin Lakes, NJ, USA), Greiner Bio-One (Kremsmünster, Austria), Sarstedt (Nümbrecht, Germany) and TPP (Trasadingen, Switzerland).

II.1.2 Chemicals and reagents

Table II-2: Chemicals and reagents.

Name	Manufacturer
4',6-Diamidino-2-phenylindole (DAPI)	Merck Millipore, Darmstadt, Germany
Bafilomycin A	Carbosynth, Newbury, UK
Bio-Rad protein assay reagent	Bio-Rad Laboratories, Hercules, CA, USA
Bovine serum albumin (BSA)	GE Healthcare, Chalfont St Giles, UK
CutSmart™ Buffer	New England Biolabs (NEB) Ipswich, MA, USA
Dithiothreitol (DTT)	AppliChem, Darmstadt, Germany
DMEM (high glucose)	Gibco/Life Technologies, Carlsbad, CA, USA
DNA Ligase T4	NEB, Frankfurt a. M., Germany
DNA marker (1kb)	NEB, Frankfurt a. M., Germany
DNAse	NEB, Frankfurt a. M., Germany
EcoRI	NEB, Frankfurt a. M., Germany
EDTA	AppliChem, Darmstadt, Germany
Ethidium bromide	AppliChem, Darmstadt, Germany
Fetal calf serum (FCS)	Gibco/Life Technologies, Carlsbad, CA, USA
Fluoromount™ Aqueous Mounting Medium	Sigma-Aldrich, St. Louis, MO, USA
iTaq™ Universal SYBR® Green Supermix	Bio-Rad Laboratories, Hercules, CA, USA
Kanamycin	Roth, Karlsruhe, Germany
KpnI	NEB, Frankfurt a. M., Germany
LB-broth	Roth, Karlsruhe, Germany

MACSfectin™	Miltenyi Biotec, Bergisch Gladbach, Germany
MG132	Carbosynth, Newbury, UK
Milk powder	Roth, Karlsruhe, Germany
Nucleospin® Gel and PCR clean-up	Machery-Nagel, Düren, Germany
Nucleospin® RNA II kid	Machery-Nagel, Düren, Germany
Penicillin-streptomycin	Gibco/Life Technologies, Carlsbad, CA, USA
peqGOLD TriFast	Peqlab biotechnologie, Erlangen, Germany
Protease inhibitor	Sigma-Aldrich, Taufkirchen, Germany
Protein marker	BioRad Laboratories Inc, Munich, Germany
Puromycin	Gibco/Life Technologies, Carlsbad, CA, USA
Q5® High-Fidelity DNA Polymerase	NEB, Frankfurt a. M., Germany
Roti®-Mount FluorCare DAPI	Roth, Karlsruhe, Germany
Shrimp-Alkaline-Phosphatase	NEB, Frankfurt a. M., Germany
SuperSignal® West Femto Kit	Thermo Fisher Scientific, Waltham, MA, USA
SuperSignal® West Pico Kit	Thermo Fisher Scientific, Waltham, MA, USA
TEMED	Roth, Karlsruhe, Germany
Trypsin	Gibco/Life Technologies, Carlsbad, CA, USA

All other chemicals used but not mentioned in Table II-2 were purchased from AppliChem, Sigma-Aldrich, Merck and Roth.

II.1.3 Buffers and solutions

If not otherwise specified, all buffers and solutions were prepared in highly purified water.

Table II-3: Buffers and solutions.

Buffer or solution	Composition
DNA sample buffer	75% v/v Glycerol 2 mg/ml Bromphenolblue 4 mg/ml Xylene cyanol 50mM EDTA
ECL solution	1250 µM 3-Aminophtalhydrazide (Luminol) 200 µM p-Coumaric acid 100 mM Tris-HCl pH 8.5 added freshly: 0.01% H_2O_2
Lysis buffer	50 mM Tris-HCl pH 7.5 150 mM NaCl 2 mM EDTA pH 8 1% NP-40
PBS	150 mM NaCl 20 mM NaH_2PO_4
Ponceau staining solution	0.1% Ponceau 5% Acetic acid
Running buffer for electrophoresis	192 mM Glycin 25 mM Tris-Base 0,1% SDS
SDS electrophoresis buffer	192 mM Glycine 25 mM Tris 0.1% SDS
SDS loading buffer (4x)	250 mM Tris-HCl pH 6.8 8% SDS 40% Glycerol 0.2% Bromphenolblue added freshly: 100 mM DTT
SOC medium	40 mM Glucose in LB medium
TAE	40 mM Tris 20 mM Acetic acid 1 mM EDTA

TBS-T	100 mM Tris-HCl pH 7.4 150 mM NaCl 0.05% Tween-20
Transfer buffer	192 mM Glycine 25 M Tris 10% v/v Methanol

II.1.4 Primary and secondary antibodies

Primary antibodies used for Western blot were diluted in TBS-T (pH 7.4) supplemented with 2.5% milk powder. Primary antibodies for immunofluorescence were diluted in PBS supplemented with 1% bovine serum albumin (BSA).

Table II-4: Primary antibodies.

Antibody	Source	IgG	WB	IF	Manufacturer
Flotillin-1	ms	mAb	1:1,000	1:25	BD Biosciences, Franklin Lakes, NJ, USA
Flotillin-2	ms	mAb	1:1,000	-	BD Biosciences, Franklin Lakes, NJ, USA
Flotillin-2 (C-terminal)	rb	pAb	-	1:100	Sigma-Aldrich, St. Louis, MO, USA
M3R	rb	pAb	1:1,000	-	Santa Cruz Biotechnology, Santa Cruz, CA, USA
tEGFR (1F4)	ms	mAb	1:1,000	-	Cell Signaling Technology, Danvers, MA, USA
pEGFR (Tyr1173)	rb	mAb	1:1,000	-	Cell Signaling Technology, Danvers, MA, USA
tERK2	rb	pAb	1:1,000	-	Santa Cruz Biotechnology, Santa Cruz, CA, USA
pERK1/2 (Tyr204)	ms	mAb	1:1,000	-	Santa Cruz Biotechnology, Santa Cruz, CA, USA
PARP-1	rb	mAb	1:1,000	-	Cell Signaling Technology, Danvers, MA, USA
GAPDH	ms	mAb	1:10,000	-	Abcam, Cambridge, UK

Secondary antibodies for Western blot were diluted in TBS-T (pH 7.4). Secondary antibodies for immunofluorescence were diluted in PBS supplemented with 1% BSA.

Table II-5: Secondary antibodies.

Antibody	Source	WB	IF	Manufacturer
Anti-mouse-HRP	gt	1:10,000	-	Dako/Agilent Technologies, Santa Clara, CA, USA
Anti-rabbit-HRP	gt	1:10,000	-	Dako/Agilent Technologies, Santa Clara, CA, USA
Anti-rabbit-Alexa Fluor 488	dk	-	1:300	Life Technologies, Carlsbad, CA, USA
Anti-mouse-Cy3	gt	-	1:300	Dianova, Hamburg, Germany

II.2 Cell biological methods

II.2.1 Cultivation of eukaryotic cells

HeLa cells (ATCC, Rockville, MD, USA) were cultivated in Dulbecco's modified Eagle's medium (DMEM) high glucose supplemented with 10% fetal calf serum (FCS), 100 U/ml penicillin and 100 µg/ml streptomycin (=DMEM++) in a humidified incubator at 37°C and 8% CO_2. Stable flotillin knock-down cell lines, used as reference in some experiments, such as sh-F2-A and sh-control (Babuke et al. 2009) received puromycin (2 µg/ml) to maintain the selecting conditions.

When the cells reached confluence, splitting was performed by washing in phosphate buffered saline (PBS) and treatment with 0.25% trypsin supplemented with 0.05% ethylenediaminetetraacetic acid (EDTA) in PBS for 5 minutes in the incubator. After addition of fresh DMEM, the cells were resuspended, and the surplus was discarded.

II.2.2 Cell transfection

Approximately 100,000 cells were seeded in a well of a 12 well plate with 1 ml cell medium. On the next day, the transfection was performed using MACSfectin™ Reagent according to the manual instructions. The ratio of µg transfected DNA to µl MACSfectin™ Reagent was 1:4. For 12-wells, 0.5 and 1 µg plasmid per well were used for the transfection with gRNA-plasmids. The gRNAs were cloned into a pD1301-AD plasmid and were obtained from Horizon Discovery Group **(**Cambridge, United Kingdom).

Table II-6: gRNA sequences.

Gene name	Abbreviation	Guide ID	gRNA sequence (5'-3')
Flotillin-1 (*FLOT1*)	G-16	165719	ATGGTTCAGGCTGGAGCTGG
	G-17	165720	TTTCACTTGTGGCCCAAATG
	G-18	165721	GTACTTACCGGAGACCACCA
	G-19	165722	GCAGAACCCTGCAAGGTGTG
	G-20	165723	CTCCAGCCACCATGACTGGG
Flotillin-2 (*FLOT2*)	G-21	126664	GCAATTGCCCATGGCGCCGG
	G-22	126665	GAAACCACCAGCGCCTCGTT
	G-23	126666	AAACACGTACTGTTTATAGT
	G-24	126667	GGAGATACACCACCAGGCCC
	G-25	126668	GACACTCAGAGGTAAGCACC

II.2.3 Single cell dilution

Since the transfection and the subsequent gene editing in the transfected cell is not successful in 100% of the target cells, a selection has to be achieved by a single cell dilution. The effect of gRNA-mediated knock-out was detected by Western blot in every transfected cell pool before a single cell dilution was performed. The most promising pools were seeded as single cell clones into a 96 well plate. Cells in trypsinised suspension were counted by means of a hemocytometer. The suspension was diluted to 1, 2 or 4 cells in 200 µl medium. Each well received 200 µl of the diluted suspension. Only those wells containing one cell colony were used for further characterisation. When the density of this

colony was high enough, the cells were transferred onto larger dishes. For screening, each single cell clone was seeded onto two 6-wells for clone expansion.

II.2.4 Storage of cells

The resuspended cells were transferred into a 15 ml tube. After centrifugation for 5 minutes at 1100 rpm, the cell pellet was resuspended in 1 ml FCS supplemented with 10% dimethyl sulfoxide (DMSO) and stored in cryo vials at -150°C.

II.2.5 Treatment with growth factors and staurosporin

Before treatment with EGF and staurosporin (STS), the cells must have reached 60 - 80% confluence and be starved in serum-free medium overnight (approximately 16 h). The stimulation with EGF (working concentration = 100 ng/ml) was performed for 10 minutes, and the treatment with staurosporin (working concentration = 1 µM) was performed for 4 hours. The control cells were kept under the starving conditions without the substances. Five independent test series were performed and analysed together.
For protein degradation analysis, the lysosomal acidification was inhibited with 50 nM bafilomycin A, and the proteasome activity was inhibited with 10 µM MG132 for 24 h in DMEM++.

II.3 Protein biochemical analysis

II.3.1 Cell lysis

Every step was performed at low temperature, on ice, and in precooled devices. Before lysis with the lysis buffer, the cells were washed in PBS. The lysis buffer was freshly supplemented with a protease inhibitor cocktail (1:100) and, for detection of phosphorylated proteins, also with sodium orthovanadate (1 mM) and sodium fluoride (1 mM). The cells were removed with a cell scraper and transferred into a new 1.5 ml tube. The cells were lysed for 20 minutes on ice and vortexed every 5 minutes. The remaining

cellular debris was removed by centrifugation (4°C, 15,000 rpm for 10 minutes) and the clear supernatant was transferred into a new 1.5 ml tube.

II.3.2 Preparation for SDS-PAGE

The protein concentrations were measured with the Bio-Rad protein assay reagent according to the manufacturer's protocol. Equal protein amounts diluted in H_2O and 25 µl SDS loading buffer (4x) were heated to 94°C for 5 minutes.

II.3.3 SDS-PAGE and Western blot

The sodium dodecyl sulphate-polyacrylamide gel electrophoresis (SDS-PAGE) was performed as a discontinuous gel electrophoresis including a stacking and a running gel. The electrophoresis chamber contained SDS electrophoresis buffer and was connected to 15 mA/gel during the stacking gel and 25 mA/gel during the running gel. Every gel was loaded with the Bio-Rad protein marker to visualise the molecular weights of standard proteins.

Table II-7: Layout for four 10% polyacrylamide gels.

Reagent	**Stacking gel**	**Running gel**
ddH_2O	11.7 ml	21 ml
3 M Tris-HCl pH 8.8	-	5 ml
3 M Tris-HCl pH 6.8	624 µl	-
20% SDS	75 µl	200 µl
Acrylamide	2.55 ml	13.4 ml
10% APS	75 µl	400 µl
TEMED	22.5 µl	64 µl
Total	15 ml	40 ml

The transfer was performed by means of Western blot at 400 mA for 1 hour onto a nitrocellulose membrane. The success of transfer was monitored with Ponceau S.

II.3.4 Immunodetection

The first step was blocking with 5% milk powder in Tris-buffered saline-Tween 20 (TBS-T) for at least 30 minutes, followed by incubation with the primary antibody overnight at 4°C. The next day, at least 3 washing steps in TBS-T each for 10 minutes were carried out. The incubation with the secondary antibody was performed for 1 hour at room temperature, followed by at least 3 washing steps in TBS-T for 10 minutes each.
The detection was performed via ECL solution. Weak signals were detected by a mixture of SuperSignal® West Femto Trial Kit and SuperSignal® West Pico Trial Kit (1:2). The exposure duration was adjusted to the signal strength.
To detect other proteins on the same membrane, blots were incubated in 0.1 M NaOH for 10 – 20 minutes, blocked with milk again and incubated with the relevant antibodies.

II.4 Molecular biological methods

II.4.1 RNA/DNA isolation and reverse transcription

The cells were grown in 12-well or 6-well plates. After washing in PBS, the cells were covered with 800 µl peqGOLD TriFast™ for 5 minutes at room temperature. The manual instructions were followed but the sample volumes were adjusted according to the volume of peqGOLD TriFast™. To purify the samples from persisting traces of DNA residues, a DNase digestion was performed:

50 µl RNA sample
10 µl Reaction buffer (10x)
1 µl DNase (=2 U)
39 µl H_2O

The reaction mixture was incubated for 10 minutes at 37°C. The subsequent inactivation of DNase was performed by adding 2.5 µl EDTA (final 5 mM) and heating to 75°C for 10 minutes. After the DNase digestion, 2 µl of the RNA-sample were pipetted onto the

NanoQuant plate™ to measure the RNA concentration by use of the Tecan Infinite M200 plate reader.

3 µg RNA sample were diluted to a volume of 19.5 µl by addition of DEPC water. If the RNA concentration was not high enough, the process was continued with 19.5 µl sample. Annealing was performed with 1.5 µl oligo dT primer (c = 1 pmol/µl) at 72°C for 4 minutes. The samples were cooled to 37°C and 24 µl of the master mix (3 µl dNTP + 4.5 µl 10xNEB reaction buffer + 0.75 µl RNAse inhibitor + 0.5 µl m-mLV reverse transcriptase + 15.25 µl DEPC water = 24 µl) was added and incubated for 2 hours at 37°C. The enzyme was inactivated by heating to 94°C for 10 minutes.

For cloning purposes, the RNA was purified by means of the Nucleospin® RNA II kit and the reverse transcription was performed with SuperScript™ III reverse transcriptase according to the manual instructions.

The isolation of genomic DNA was performed following the manual instructions of TriFast™ for DNA isolation.

II.4.2 Quantitative real-time PCR

The samples were always analysed as duplicates to minimise pipetting errors. Every well of a qPCR plate or stripe was filled with 3.8 µl DEPC water, 0.8 µl cDNA and 5.4 µl master mix (0.2 µl of 20 µM forward primer + 0.2 µl of 20 µM reverse primer + 5 µl 2x iTaq™ Universal SYBR® Green Supermix).

Table II-8: Sequences of the qPCR primers.

Target gene	Primer name	Sequence 5'-3'
FLOT1	Flot1-exon10-fwd	TATGCAGGCGGAGGCAGAAG
	Flot1-exon12-rev	CAGTGTGATCTTATTGGCTGAA
FLOT2	Flot2-exon8-fwd	GAGATTGAGATTGAGGTTGTG
	Flot2-exon9-rev	ATCCCCGTATTTCTGGTAGG
RPL13A	Rpl13a-fwd	CCTGGAGGAGAAGAGGAAAGAGA
	Rpl13a-rev	TTGAGGACCTCTGTGTATTTGTCAA
B2M	B2M-fwd	AGATGAGTATGCCTGCCGTGTG
	B2M-rev	TGCGGCATCTTCAAACCTCCA

YWHAZ	Ywhaz-fwd	AGGTTGCCGCTGGTGATGAC
	Ywhaz-rev	GGCCAGACCCAGTCTGATAGGA

The following qPCR program was used:

95°C	10 min	
95°C	15 sec	39x
60°C	30 sec	
72°C	30 sec	
95°C	10 min	

II.4.3 Cloning

For the examination of DNA and cDNA sequences of flotillin-1 and flotillin-2 in the knock-out cell clones, the respective gene area was PCR-amplified using the Q5® High-Fidelity DNA Polymerase:

2 µl	Template DNA/cDNA (c = 150 ng/µl)
20 µl	5x Q5 buffer
2 µl	dNTPs (10 mM)
1 µl	Forward primer (100 µM)
1 µl	Reverse primer (100 µM)
1 µl	Q5® High-Fidelity DNA Polymerase
73 µl	DEPC H_2O

The primer sequences were designed from the start codon to stop codon for cDNA. Since the gene area on the genomic DNA is too long for a complete amplification, the primers were designed around the gRNA binding site, were the DSB was expected. The primers were provided with recognition sites for the restriction enzymes KpnI and EcoRI.

Table II-9: Primer sequences used for cloning of the genomic DNA and cDNA fragments into a plasmid for sequencing purpose.

Primer name	**Sequence 5'-3'**
hFlot-1-genomic-fwd	CTATA *GGTACC* TCCCTCTCCCTACCAACTTCCC
hFlot-1-genomic-rev	CTATA *GAATTC* TGCAGGCAAGGGTTGAGAAGAC
hFlot-1- cDNA-fwd	CTATA *GGTACC* ATGTTTTTCACTTGTGGCCC
hFlot-1-cDNA-rwd	CTATA *GAATTC* CCGGCTGTTCTCAAAGGCTTG
hFlot-2-genomic-fwd	CTATA *GGTACC* ATCACCTCTGCCCATTGTCCT
hFlot-2-genomic-rev	CTATA *GAATTC* CCTTCCTGATGCATGTCTCCTG
hFlot-2- cDNA-fwd	CTATA *GGTACC* ATGGGCAATTGCCACACGG
hFlot-2-cDNA-rwd	CTATA *GAATTC* CCCACCTGCACACCAGTGGC

The following PCR-program was used:

98°C	30 sec	
98°C	10 sec	⎫
58°C – 65°C*	30 sec	⎬ 30 times
72°C	30 sec	⎭
72°C	2 min	

* annealing temperature was determined by the NEB Tm Calculator (www. tmcalculator.neb.com)

The amplified PCR products were separated via gel electrophoresis in a 1% agarose gel with ethidium bromide (1:10,000). The samples were prepared with 6x DNA sample buffer and the electrophoresis was performed at 100 mV.
If there was one clear band, no purification was performed. In other cases, the relevant parts were cut out, and the PCR products were extracted by means of the NucleoSpin® Gel and PCR Clean-up.

The amplified flotillin inserts were to be cloned into a pEGFP-N1 vector. For the restriction digestion, the samples were incubated in a 0.5 ml tube over night at 37°C:

7 µl CutSmart™ Buffer (10x)
2 µl EcoRI (10 U/µl)
2 µl KpnI (10 U/µl)
PCR product or 10 µg pEGFP-N1
Add H_2O to 70 µl

The removal of 5'-phosphates in pEGFP-N1 was performed using the Shrimp-Alkaline-Phosphatase for 3 hours at 37°C:

3µl rSAP
Plasmid restriction digestion
Add 10x rSAP buffer according to volume

The T4 ligase was used to ligate insert restriction digestion and plasmid restriction digestion:

4 µl Insert restriction digestion
4 µl Plasmid restriction digestion (approx. 500 ng)
1 µl 10x T4 buffer
1 µl Ligase T4

The incubation was performed at 16°C overnight. Amounts of the insert and the plasmid were adjusted for optimal ligation and transformation result. At the end of each step, the enzymes were heat inactivated for 10 minutes at 65°C.

II.4.4 Transformation and plasmid purification

Aliquots of competent XL1-Blue (Stratagene, La Jolla, CA, USA) are stored at -80°C. The following steps were performed:

1. Bacteria and 5 µl ligation product were transferred into a 1.5 ml tube and preincubated for 30 minutes on ice.
2. Heat shock at 45°C for 90 seconds
3. 1 minute on ice
4. Add 1 ml SOC medium
5. Shaking for 45 minutes at 37°C, 220 rpm
6. Plate on an agar plate considering antibiotic resistance over night at 37°C

The single colonies were selected and inoculated in LB medium containing the appropriate antibiotic at 220 rpm and 37°C over night.

The plasmid purification was performed by means of Nucleospin® Plasmid according to the manual instructions. After measuring the DNA concentration via NanoQuant plate™ and Tecan Infinite M200 plate reader, the restriction digestion was performed:

3 µl Plasmid (c = 75 ng/µl)
1 µl CutSmart™ Buffer (10x)
0.2 µl KpnI (10 U/µl)
0.2 µl EcoRI (10 U/µl)
5.6 µl H_2O

The incubation was performed for 2 h at 37°C. Then the digested product was separated in an agarose gel electrophoresis to visualise the success of cloning. The purified plasmids were adjusted according to the requirements of Eurofins genomics sequencing service and send off.

II.5 Microscopy

II.5.1 Seeding of cells on coverslips

Every well of a 12 well plate received one coverslip (⌀ = 13 mm). The cells were seeded in the wells and grown to 80 – 100% confluence.

II.5.2 Transfection efficiency control by GFP

All gRNA-plasmids carry a green fluorescent protein (GFP) sequence, to enable a control of transfection success. The coverslips colonised by the recently transfected cells were washed in PBS and fixed with 4% paraformaldehyde (PFA) at 37°C in an incubator for 10 minutes. After washing two times with PBS, the coverslips were mounted on glass slides with Roti®-Mount FluorCare DAPI.

II.5.3 Immunofluorescence

Two washing steps in PBS were performed before the fixation with methanol for 10 minutes at -20°C. Washing was repeated to remove methanol residues. The coverslips were transferred into a humid chamber, and blocking was performed with 30 µl 1% BSA in PBS for 10 minutes at room temperature. The incubation with the primary antibody was carried out for 1 hour at room temperature.

Then the coverslips were washed three times for at least 10 minutes with PBS. After the washing, the incubation with the secondary antibody was performed in the humid chamber at the same conditions as the primary antibody incubation. The antibody solution received, beside the appropriate secondary antibodies, DAPI (1:1000). The secondary antibody incubation was followed by washing with PBS in the 12 well plate. To remove salt crystals, the coverslips were cleaned quickly with purified water, before the fixation on glass slides with Fluoromount™ Aqueous Mounting.

II.6 Statistical analysis and image preparation

For statistical analysis, all experiments were performed at least 3 times. Protein quantification in Western blot was performed by means of the Quantity One software (Bio-Rad Laboratories, Hercules, CA, USA). Microsoft Excel was used for analysis and to create diagrams. The figures were generated by CorelDRAW X4 (Corel Corporation, Ottawa, Canada) and Microsoft PowerPoint. Image preparation was performed by Adobe Photoshop CS4 (Adobe Systems, San Jose, CA, USA). In some images, brightness, contrast and tonal value were adjusted. The microscopic images were exported as Tagged Image File Format (tif) from the ZEN software (Zeiss, Oberkochen, Germany). *In silico* translation was performed by the ExPASy Translate tool (https://web.expasy.org/translate). Alignment of DNA and cDNA sequences to the relevant refseq was analysed with BLAST® (NCBI) (https://blast.ncbi.nlm.nih.gov).

III. Results

III.1 Generation of knock-out cell lines

III.1.1 Transfection of HeLa cells

The plasmids encoding a GFP-tagged Cas9 enzyme and gRNAs targeting human flotillin-1 and -2 were obtained through the Horizon genome project, and HeLa cells were transfected with the plasmids. Toleration of the transfection procedure, observed as survival of the cells, differed depending on the gRNA that was used. In the first trial for flotillin-2, cell pools transfected with the gRNAs G-21 and G-22 did not survive the transfection, indicating that the concerning off-target effects may compromise cell survival. The transfection success was controlled by monitoring the Cas9-GFP expression by fluorescent microscopy (Figure III-1) and by Western blot (Figure III-2) in order to detect the most promising cell pools that were used for the subsequent single cell dilution.

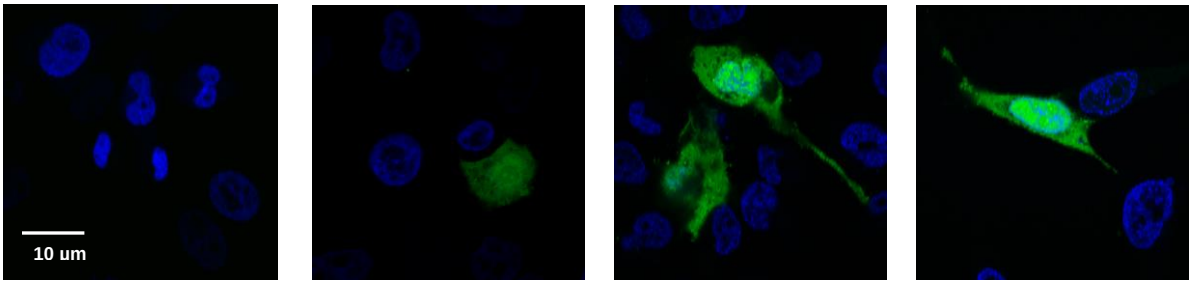

Figure III-1: Transfected HeLa cell pools for flotillin-2 knock-outs stained with DAPI (blue). Cells with successful transfection of the gRNA/Cas9 plasmid express GFP and appear green.

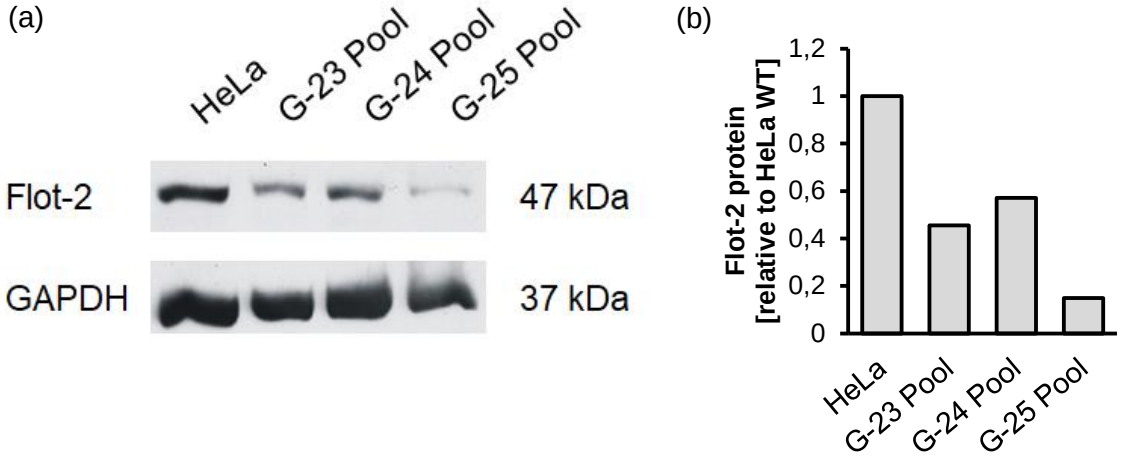

Figure III-2: (a) Western blot detection of transfected cell pools with flotillin-2 knock-out. **(b)** Densitometric quantification of flotillin-2 signals normalised to GAPDH. The values are shown as relative to HeLa WT. Compared to HeLa WT, all cell pools show a reduced expression level of flotillin-2. The G-23 and G-25 Pools present the highest reduction of flotillin-2 and were thus selected for the generation of single cell clones.

The transfection success for flotillin-1 knock-outs and for double knock-outs (negative for both flotillins) was controlled in the same way as above and showed similar results. In all cases, the most promising cell pools were chosen for single cell dilution.

III.1.2 Detection of the knock-out single cell clones

Single cell clones from the most promising cell pools were obtained by limiting dilution, and protein expression was detected by Western blot (Figure III-3). In the case of flotillin-1 (F1-KO) and flotillin-2 (F2-KO) knock-out, several cell clones without detectable flotillin protein expression were generated. Double-knock-out cell lines negative for flotillin-1 and flotillin-2 were generated by transfecting the F1-KO clone 2 and the F1-KO clone 7 with gRNA plasmids targeting flotillin-2. An overview of all created knock-out cell lines can be found in Table III-1.

In some cases (F1-KO clone X or F2-KO clone 3), the expression of the targeted flotillin emerged again after a few passages, caused most likely due to incomplete single cell dilution. The growth rate differed between the cell clones, with some clones showing very low growth rates, and these clones were thus not used for further analysis.

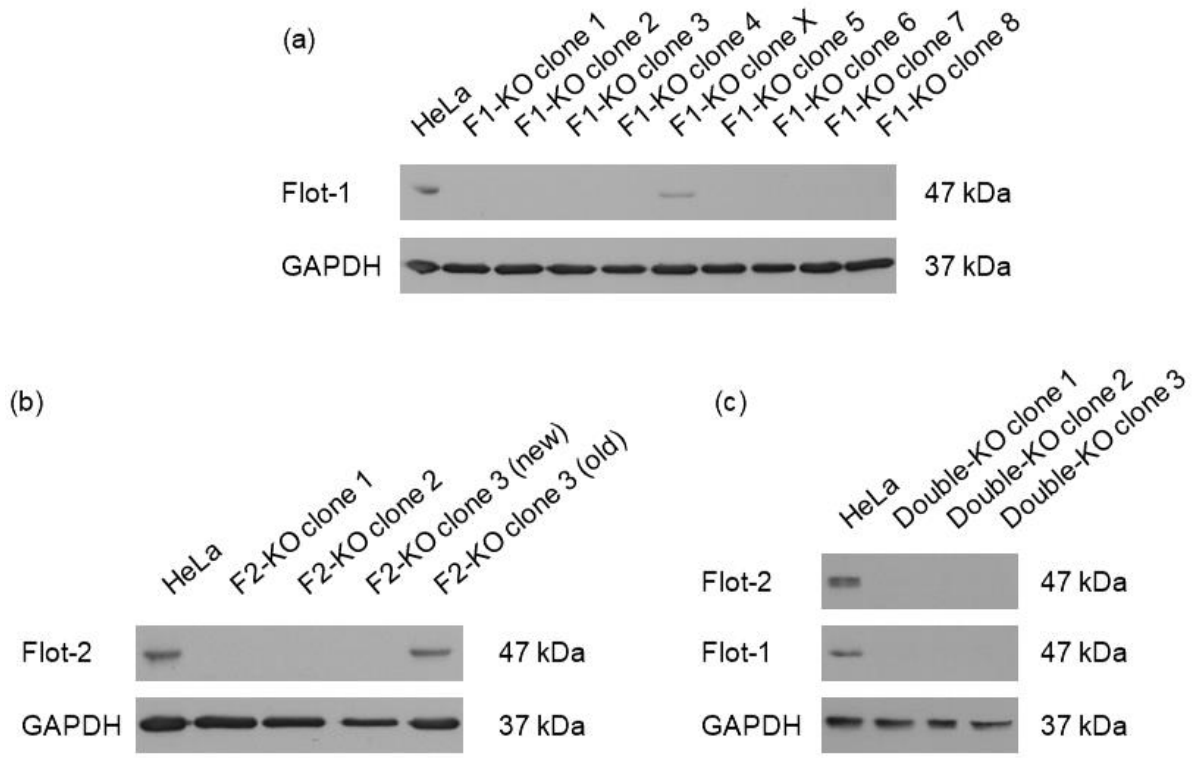

Figure III-3: Validation of the knock-out cell lines on protein level with Western blot. **(a)** Flotillin-1 knock-outs, all clones except F1-KO clone X do not show any flotillin-1 expression. **(b)** Flotillin-2 knock-outs, the F2-KO clone 3 showed flotillin-2 expression after ≈ 10 passages. **(c)** Double-knock-out cell lines show absence of both flotillins.

To reduce the workload for further analysis, only the clones F1-KO clone 2, F1-KO clone 7, F2-KO clone 2, double-KO clone 1, and double-KO clone 2 were used.

Table III-1: Flotillin knock-out cell lines.

	Nomenclature	gRNA used	Comment
Flotillin-1-KO	F1-KO clone 1	G-20	
	F1-KO clone 2	G-20	
	F1-KO clone 3	G-20	
	F1-KO clone 4	G-20	
	F1-KO clone 5	G-20	
	F1-KO clone 6	G-20	
	F1-KO clone 7	G-20	
	F1-KO clone 8	G-20	

Flotillin-2-KO	F2-KO clone 1	G-22	
	F2-KO clone 2	G-22	
	F2-KO clone 3	G-25	Only 10 passages
Double-KO	Double-KO clone 1	G-20, G-25	F1-KO clone 7 transfected with G-25
	Double-KO clone 2	G-20, G-25	
	Double-KO clone 3	G-20, G-25	

III.2 Analysis of the flotillin knock-out clones

III.2.1 Response to treatment with Staurosporin and EGF

Many recent studies have shown an involvement of flotillins in transduction of growth factor signals and in apoptosis. However, in some cases, contradictory results have been reported due to the use of various cell systems and different degrees of flotillin depletion. Thus, the aim was to analyse the effects of a complete flotillin knock-out on signalling in human cells. HeLa wild-type and the knock-out cell lines generated above were treated with EGF and staurosporin. Staurosporin is an inducer of cell cycle arrest and apoptosis through Caspase-3 activation. This activation leads to proteolytic degradation of PARP-1, which can be quantified. Percentage of cleaved PARP-1 after treatment with staurosporin is shown in Figure III-4b. In none of the investigated single knock-out cell lines, significant differences were detected compared to HeLa wild-type. A significant augmentation of PARP-1 cleavage could only be detected in double-KO clone 1. Figure III-4a demonstrates one representative Western blot out of five experiments, the quantitative analysis of which is shown in Figure III-4b.

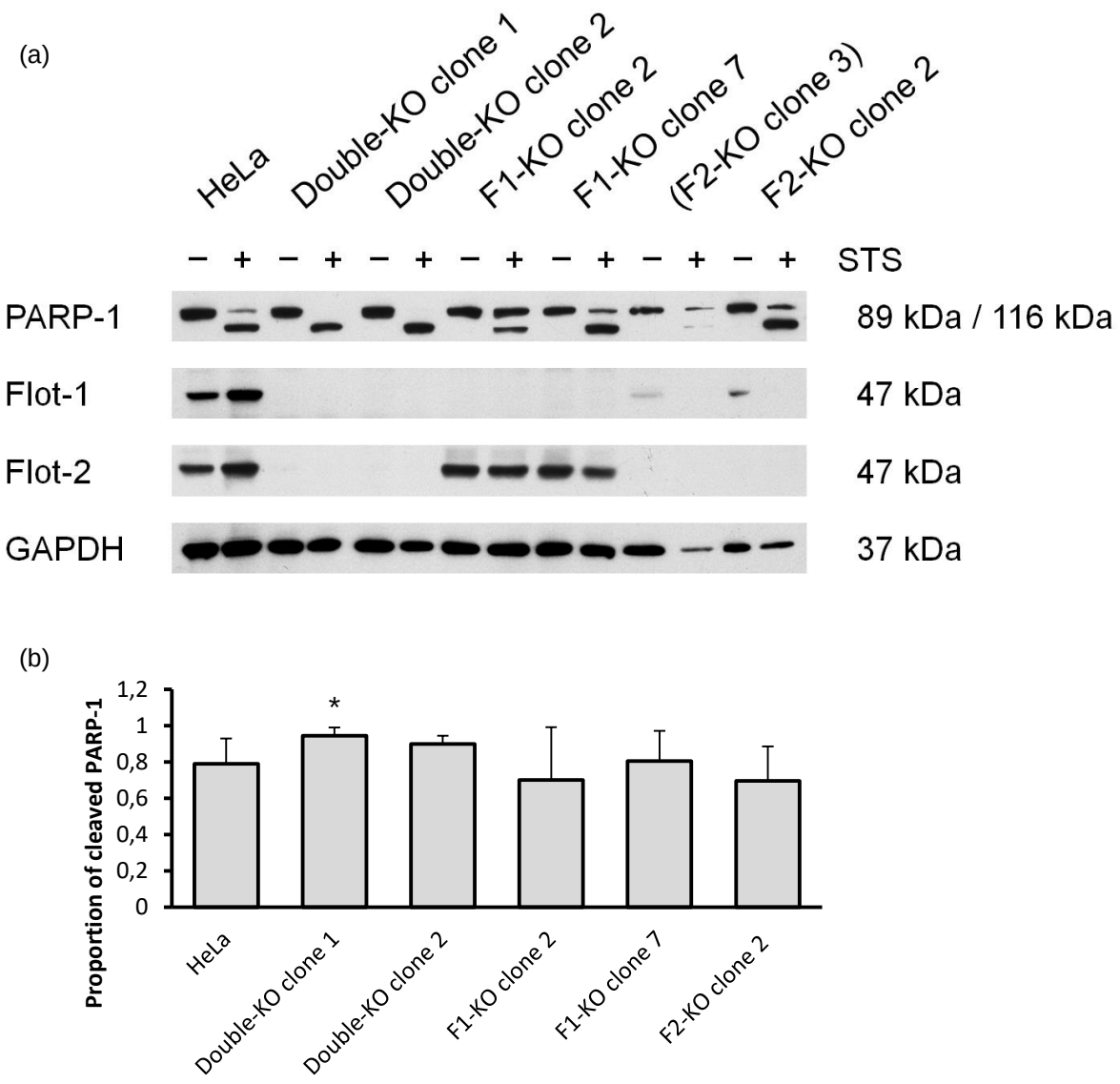

Figure III-4: (a) Apoptosis induction in flotillin knock-out cells. HeLa WT and knock-out cell lines were starved overnight, treated with 1 µM staurosporin for 4 h, and apoptosis induction was detected through appearance of cleaved PARP-1. The antibody against PARP-1 detects the cleaved and uncleaved protein. **(b)** Quantification of cleaved PARP-1 in proportion to total PARP-1 after treatment with staurosporin. Five independent experiments were performed and analysed together. Significant results are marked with * ($p < 0.05$).

EGF stimulation of cells leads to a phosphorylation of the EGF receptor and an activation of the downstream ERK signalling. Five independent experiments were performed, of which one representative Western blot is shown in Figure III-5a. The densitometric quantification of the phosphorylation of ERK is depicted in Figure III-5b. The absence of

flotillins does not seem to have a significant impact on the EGF-induced phosphorylation of ERK and EGFR.

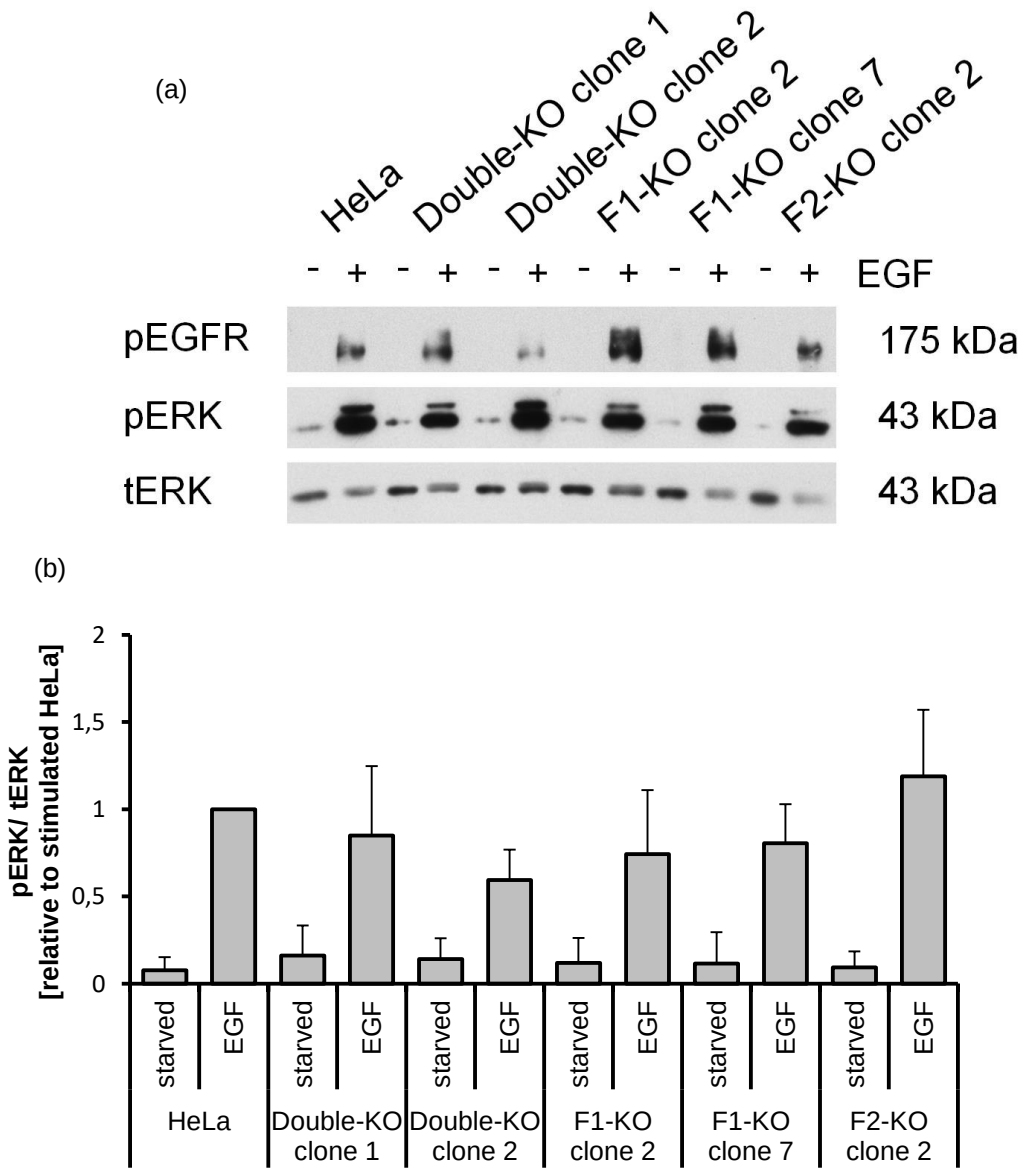

Figure III-5: (a) One out of five representative Western blots. EGF-stimulated cells activate a signalling cascade phosphorylating the EGF-receptor and downstream proteins such as ERK. **(b)** Densitometric quantification of pERK normalised to tERK (total ERK). Mean values of five experiments are represented relative to EGF-stimulated HeLa.

III.2.2 Microscopy

Immunofluorescence microscopy was used to analyse the expression and distribution of flotillins. In HeLa wild-type cells, a specific flotillin signal was found at the plasma membrane, where both flotillin-1 and -2 colocalise, as well as in intracellular vesicles. In F1-KO clone 2 and F1-KO clone 7, flotillin-2 was still located at the plasma membrane and in intracellular vesicles, whereas antibodies against flotillin-1 only exhibited a slight, homogeneous background signal. Similarly, in F2-KO clone 2, flotillin-1 was found at the plasma membrane and in intracellular vesicles, while flotillin-2 could not be detected. In the double-KO clone 1 and double-KO clone 2, there was no specific signal for both flotillins, demonstrating the knock-out of both proteins (see Figure III-6).

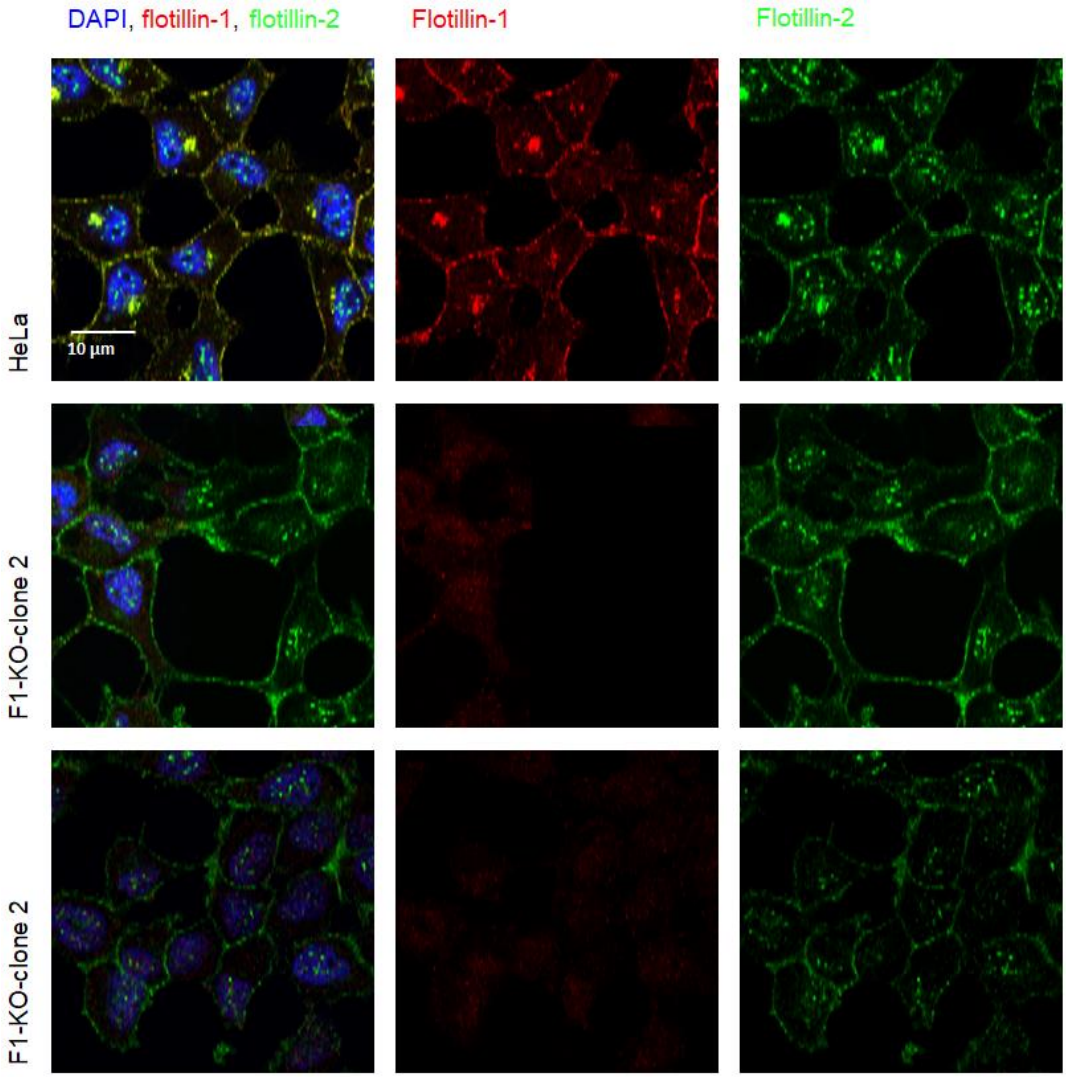

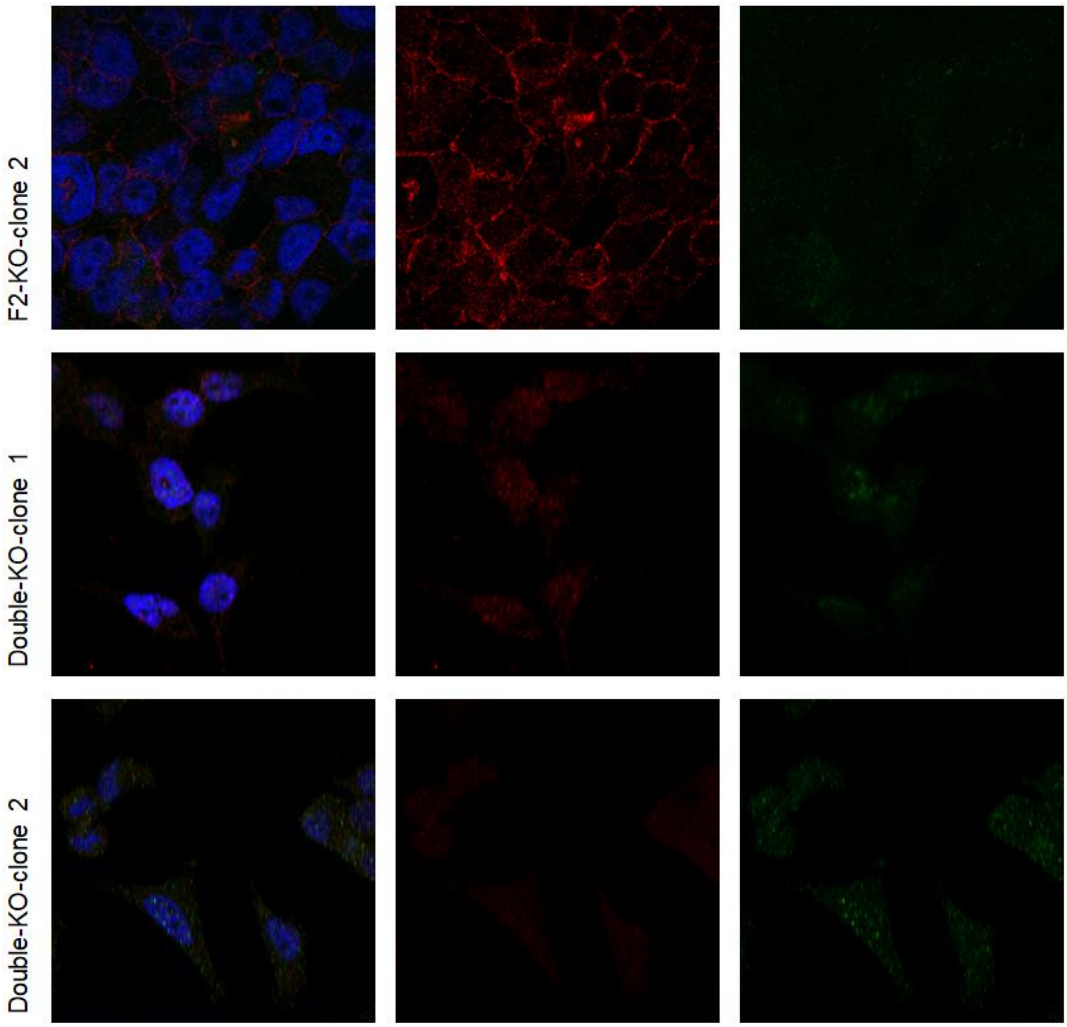

Figure III-6: Immunofluorescence microscopy of HeLa wild-type and knock-out cell lines. Flotillins are situated at the plasma membrane and in intracellular vesicles. HeLa wild-type cells show positive signals for both flotillins and DAPI. Flotillin-1 knock-out cell lines do not have a positive signal for flotillin-1. Flotillin-2 remains in the plasma membrane and intracellular vesicles. Similarly to that, F2-KO clone 2 has no positive signal for flotillin-2 but flotillin-1 resides in vesicles and plasma membrane. The double knock-out cell lines did not show any positive signal for any flotillin.

III.2.3 Quantitative real-time PCR

Since CRISPR-Cas9 mainly causes minor alterations (indels) in the genomic DNA, the transcription of the gene and the amount of mRNA should not be affected, in contrast to siRNA-mediated knock-down. Relative amounts of flotillin-1 and flotillin-2 mRNA in F1 and F2 knock-out cell lines as well as sh-F2-A with a stable shRNA knock-down of flotillin-2 were compared to HeLa cells (knock-out cell lines) or HeLa cells with a control shRNA (knock-down cells) and are shown in Figure III-7.

The knock-out cell lines showed some differences in the amount of flotillin mRNA, as compared to wild-type HeLa cells. In flotillin-1 knock-outs, the mRNA levels for flotillin-1 range from 18 to 112%, whereas in flotillin-2 knock-outs, the mRNA levels for flotillin-2 range from 41 to 102%. However, the mRNA levels of the other flotillin were not substantially affected by the knock-out of its counterpart. The two knock-out cell lines F1-KO clone 2 and F1-KO clone 8 showed the highest reduction of F1-mRNA, up to 18%, which could be due to mRNA instability.

Since RNA interference with shRNAs reduces the amount of the corresponding mRNA, sh-F2-A shows a substantial reduction of flotillin-2 mRNA, which subsequently is responsible for the reduced protein translation.

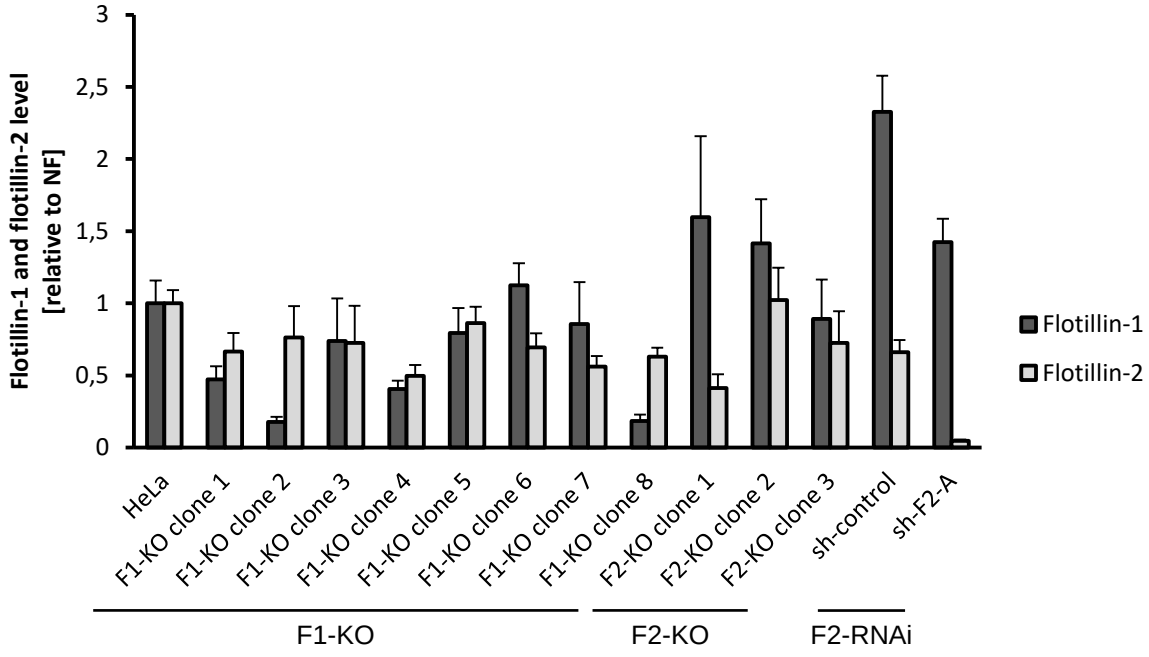

Figure III-7: Relative levels of mRNA for flotillin-1 and flotillin-2. Quantitative real-time PCR was performed for HeLa wild-type, knock-out cell lines and for the stable flotillin-2 knock-down (sh-F2-A) and control shRNA HeLa cells. Dark-grey bars show flotillin-1 mRNA levels, light grey bars flotillin-2 mRNA. Values are mean of two samples per clone.

III.2.4 Sequencing

To characterise the exact genomic changes caused by the knock-out procedure, sequencing of genomic DNA was performed with double-KO clone 1 and double-KO clone 2 for *FLOT1* and *FLOT2*, as well as with F1-KO clone 2 and F1-KO clone 7 for *FLOT1*. Since HeLa cells are hypertriploid (Landry et al. 2013) and thus exhibit at least three copies of chromosomes 6 and 17, on which *FLOT1* and *FLOT2* are located, one can expect three or even more possible genomic mutation variants in each single cell clone, depending on the HeLa cell subgroup. Primers for PCR amplification of the genomic region were designed on both sides of the target site of the respective gRNAs, since the whole gene is too long for amplification (amplicon length for *FLOT1*: 576 bp, *FLOT2*: 589 bp). The primers for amplification of the cDNA were designed from the start to the stop codon. The resulting PCR products were cloned into a plasmid for sequencing. Three independently prepared samples were analysed for each cell line.

Sequencing results of the cloned fragments showed, as expected, indel mutations from one up to 35 base pairs in length at the typical locations around the gRNA binding area. Figure III-8 demonstrates the mutations of the two double-knock-out cell lines for *FLOT2*. In one case, a deletion covering 35 bp was observed (Figure III-8b).

(a) Double-KO clone 1 (flotillin-2)

1) Deletion of 14 bp

```
RefSeq 28888916  GACAGGTCCTAGAGCCCCCAGGTGCTTACCTCTGAGTGTCGGAGATACACCACCAGGCCC  28888975
                 ||||||||||||||             ||||||||||||||||||||||||||||||
Clone  295       GACAGGTCCTAGAG-------------CCTCTGAGTGTCGGAGATACACCACCAGGCCC  340
```

2) Deletion of 12 bp

```
RefSeq 28888916  GACAGGTCCTAGAGCCCCCAGGTGCTTACCTCTGAGTGTCGGAGATACACCACCAGGCCC  28888975
                 ||||||||||||||             ||||||||||||||||||||||||||||||
Clone  294       GACAGGTCCTAGAGCC------------CCTCTGAGTGTCGGAGATACACCACCAGGCCC  341
```

(b) Double-KO clone 2 (flotillin-2)

1) Deletion of 3 bp

```
RefSeq 28888916  GACAGGTCCTAGAGCCCCCAGGTGCTTACCTCTGAGTGTCGGAGATACACCACCAGGCCC  28888975
                 ||||||||||||||||||||   ||||||||||||||||||||||||||||||||||
Clone  294       GACAGGTCCTAGAGCCCCCAGG---TTACCTCTGAGTGTCGGAGATACACCACCAGGCCC  350
```

2) Deletion of 35 bp

```
RefSeq 28888901  CTGGCCCACTCCATGACAGGTCCTAGAGCCCCCAGGTGCTTACCTCTGAGTGTCGGAGAT  28888961
                 ||||||||                                  ||||||||||||||||
Clone  278       CTGGCCCA-----------------------------------CTCTGAGTGTCGGAGAT  338
```

Figure III-8: CRISPR-induced alterations of flotillin-2 genomic DNA in double-KO clone 1 and double-KO clone 2. The genomic DNA was obtained from knock-out cell lines and the area around gRNA binding site was PCR amplified and subsequently cloned into a plasmid for sequencing purposes. Two different indel mutation variants were detected in each cell clone. **(a)** Alignment of the *FLOT2* RefSeq and the genomic DNA from double-KO clone 1. Deletions of 14 and 12 bp localised close to the gRNA binding site were found. **(b)** In the genomic DNA obtained from the double-KO clone 2, the size of the deletion covered 35 bp on one allele. Another allele with a 3 bp deletion was detected as well. The alignment was performed against the *FLOT2* reference gene sequence NC_000017.11. The gRNA target site is highlighted in light blue.

In case of the F1-KO clone 2, a frameshift mutation seems to be uniformly present on all chromosomes, since an insertion of one base (A) was the only alteration detected in this cell line (Figure III-9).

Clone 2: insertion of an extra A in exon 3

```
RefSeq 893   TCCTGTGGGTTGCTGTCCCCTCACCCCCGCCAGTTCCTCAGTCTTCCACATTCAAGCTCT  952
             ||||||||||||||||||||||||||||||||||||||||||||||||||||||||||
Clone  545   TCCTGTGGGTTGCTGTCCCCTCACCCCCGCCAGTTCCTCAGTCTTCCACATTCAAGCTCT  486

RefSeq 953   GCCACCGTTCCTCACTGCCCCACACCTTGCAGGGTTCTGCCGAAGCCCCCCA-GTCATGG  1011
             |||||||||||||||||||||||||||||||||||||||||||||||||||| |||||||
Clone  485   GCCACCGTTCCTCACTGCCCCACACCTTGCAGGGTTCTGCCGAAGCCCCCCCAAGTCATGG  426

RefSeq 1012  TGGCTGGAGGGCGTGTCTTTGTCCTGCCCTGCATCCAACAGATCCAGAGGTAGGCAAGAA  1071
             ||||||||||||||||||||||||||||||||||||||||||||||||||||||||||
Clone  425   TGGCTGGAGGGCGTGTCTTTGTCCTGCCCTGCATCCAACAGATCCAGAGGTAGGCAAGAA  366
```

Figure III-9: The genomic DNA of F1-KO clone 2 showed an insertion of one A on all investigated alleles of the *FLOT1* gene. Genomic DNA was obtained from the knock-out cell line and the area around the gRNA binding site was PCR-amplified. The fragment was cloned into a plasmid for sequencing purposes. Alignment was performed with the *FLOT1* reference gene sequence NC_000006.12. The gRNA binding site is highlighted in light blue, the insertion of A is highlighted in red. (Figure from Kapahnke et al. 2016)

In the F1-KO clone 7, two different indel mutations were detected, one 17 bp deletion and another 5 bp deletion (Figure III-10). Both mutations overlap with the gRNA binding site, as it was observed for the other clones as well.

(a) Clone 7: 17 bp deletion

```
RefSeq 899   GGGTTGCTGTCCCCTCACCCCCGCCAGTTCCTCAGTCTTCCACATTCAAGCTCTGCCACC  958
             ||||||||||||||||||||||||||||||||||||||||||||||||||||||||||||
Clone  121   GGGTTGCTGTCCCCTCACCCCCGCCAGTTCCTCAGTCTTCCACATTCAAGCTCTGCCACC  180

RefSeq 959   GTTCCTCACTGCCCCACACCTTGCAGGGTTCTGCCGAAGCCCCCCAGTCATGGTGGCTGG  1018
             ||||||||||||||||||||||||||||||||||||||||||||||||||||||||||||
Clone  181   GTTCCTCACTGCCCCACACCTTGCAGGGTTCTGCCGAA----------------GCTGG  223

RefSeq 1019  AGGGCGTGTCTTTGTCCTGCCCTGCATCCAACAGATCCAGAGGTAGGCAAGAAGGGAACC  1078
             ||||||||||||||||||||||||||||||||||||||||||||||||||||||||||||
Clone  224   AGGGCGTGTCTTTGTCCTGCCCTGCATCCAACAGATCCAGAGGTAGGCAAGAAGGGAACC  283
```

(b) Clone 7: 5 bp deletion

```
RefSeq 893   TCCTGTGGGTTGCTGTCCCCTCACCCCCGCCAGTTCCTCAGTCTTCCACATTCAAGCTCT  952
             ||||||||||||||||||||||||||||||||||||||||||||||||||||||||||||
Clone  174   TCCTGTGGGTTGCTGTCCCCTCACCCCCGCCAGTTCCTCAGTCTTCCACATTCAAGCTCT  233

RefSeq 953   GCCACCGTTCCTCACTGCCCCACACCTTGCAGGGTTCTGCCGAAGCCCCCCAGTCATGGT  1012
             ||||||||||||||||||||||||||||||||||||||||||||||||||     ||||||
Clone  234   GCCACCGTTCCTCACTGCCCCACACCTTGCAGGGTTCTGCCGAAGCCCC-----CATGGT  288

RefSeq 1013  GGCTGGAGGGCGTGTCTTTGTCCTGCCCTGCATCCAACAGATCCAGAGGTAGGCAAGAAG  1072
             ||||||||||||||||||||||||||||||||||||||||||||||||||||||||||||
Clone  421   GGCTGGAGGGCGTGTCTTTGTCCTGCCCTGCATCCAACAGATCCAGAGGTAGGCAAGAAG  362
```

Figure III-10: F1-KO clone 7 showed two different mutations on the genomic DNA. Deletions of 17 bp **(a)** or 5 bp **(b)** are not multiples of 3, and they are thus expected to lead to a frameshift and loss of functional protein product. Genomic DNA was obtained from F1-KO clone 7. Area around the gRNA binding site was PCR-amplified and cloned into a plasmid for sequencing purposes. The gRNA binding site is highlighted in light blue. Alignment with the *FLOT1* reference gene sequence NC_000006.12. (Figure from Kapahnke et al. 2016)

Since frameshift mutations frequently result in an early stop codon, which can alter mRNA stability, the presence of flotillin-1 mRNA in the knock-out cells was analysed next. Reverse transcription was applied to obtain flotillin-1 cDNA from the wild-type and flotillin-1 knock-out cells, and the coding region of flotillin-1 was PCR-amplified from the cDNA.

Agarose gel electrophoresis was carried out to control the success of PCR amplification of the cDNA. Surprisingly, in addition to the expected band, additional bands on the agarose gel of PCR-amplified cDNA were observed, which might represent mRNA variants that contain deletions larger than expected to result from the indel mutations. Figure III-11 shows an agarose gel electrophoresis of HeLa cells and the two knock-out cell lines, F1-KO clone 2 and F1-KO clone 7. In the knock-out clones, two additional bands smaller than the

expected full-length mRNA of about 1400 bp were observed. To characterise the PCR products of different sizes in the flotillin-1 knock-out clones 2 and 7 (Figure III-11), the PCR products were cloned into a plasmid for sequencing.

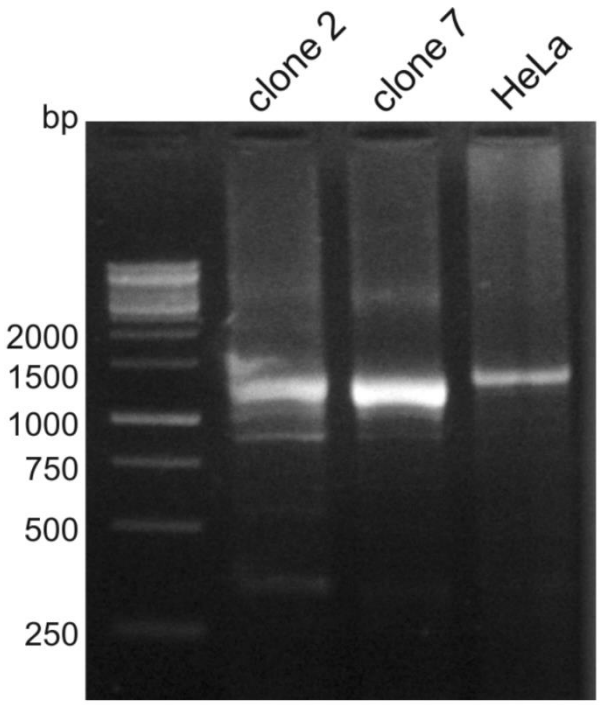

Figure III-11: Agarose gel electrophoresis of PCR-amplified flotillin-1 cDNA. The cDNA obtained from wild-type HeLa cells exhibits a single band at about 1400 bp. In addition to this major band, two smaller bands were detected in the electrophoresis of the cDNA obtained from F1-KOs clone 2 and clone 7. **(**Figure from Kapahnke et al. 2016)

The sequence analysis of cDNA from wild-type HeLa cells revealed no differences to the *FLOT1* reference sequence (Figure III-12a). In the case of F1-KO clone 2 and F1-KO clone 7, the changes based on the indel mutations detected on genomic DNA were expected to produce the respective changes in the mRNA upon transcription. However, parts of the open reading frame were missing from the cDNAs cloned from the knock-out cell lines. The missing sections corresponded to full exons that have been spliced out with the correct exon-intron borders. In Figure III-12b-e, sequence variants of flotillin-1 mRNA detected in the knock-out cells are displayed. Figure III-12b shows the expected insertion of an A within exon 3 in F1-KO clone 2, but the cDNA also lacks the complete exon 4. In another cDNA clone from F1-KO clone 2 (Figure III-12c), the complete exons 3 – 5 are missing, so

that the insertion of the extra A cannot be observed as it is located in exon 3, which has been excised. Another variant of F1-KO clone 2 is shown in Figure III-12d, with missing exon 3. The F1-KO clone 7 contains a genomic deletion of 17 bp in exon 3, which is detected in the cDNA clones, but in addition to that also exon 4 has been deleted (Figure III-12e). A cDNA clone originating from one of the other chromosomes in the same cell clone, with only a 5 bp deletion in the genomic DNA, was not detected, implicating that such mRNA species may be unstable.

(a) WT flotillin-1 sequence (coding region, exons 2-6 only)

ATGTTTTTCACTTGTGGCCCAAATGAGGCCATGGTGGTCTCCGGGTTCTGCCGAAGCCCCCCAGTCATGG
TGGCTGGAGGGCGTGTCTTTGTCCTGCCCTGCATCCAACAGATCCAGAGGATCTCTCTCAACACACTGAC
CCTCAATGTCAAGAGTGAAAAGGTTTACACTCGCCATGGGGTCCCCATCTCAGTCACTGGCATTGCCCAG
GTAAAAATCCAGGGGCAGAACAAGGAGATGTTGGCGGCCGCCTGTCAGATGTTCCTGGGGAAGACGGAGG
CTGAGATTGCCCACATTGCCCTGGAGACGTTAGAGGGCCACCAGAGGGCCATCATGGCCCACATGACTGT
GGAGGAGATCTATAAGGACAGGCAGAAATTCTCAGAACAGGTTTTCAAAGTGGCCTCCTCAGACCTGGTC
AACATGGGCATCAGTGTGGTTAGCTACACTCTGAAGGACATTCACGATGACCAG...

(b) Clone 2: insertion of an A in exon 3, exon 4 spliced out

ATGTTTTTCACTTGTGGCCCAAATGAGGCCATGGTGGTCTCCGGGTTCTGCCGAAGCCCCCCAAGTCATG
GTGGCTGGAGGGCGTGTCTTTGTCCTGCCCTGCATCCAACAGATCCAGAGGTAAAAATCCAGGGGCAGAA
CAAGGAGATGTTGGCGGCCGCCTGTCAGATGTTCCTGGGGAAGACGGAGGCTGAGATTGCCCACATTGCC
CTGGAGACGTTAGAGGGCCACCAGAGGGCCATCATGGCCCACATGACTGTGGAGGAGATCTATAAGGACA
GGCAGAAATTCTCAGAACAGGTTTTCAAAGTGGCCTCCTCAGACCTGGTCAACATGGGCATCAGTGTGGT
TAGCTACACTCTGAAGGACATTCACGATGACCAG...

(c) Clone 2: exons 3-5 spliced out

ATGTTTTTCACTTGTGGCCCAAATGAGGCCATGGTGGTCTCCGGAGATCTATAAGGACAGGCAGAAATTC
TCAGAACAGGTTTTCAAAGTGGCCTCCTCAGACCTGGTCAACATGGGCATCAGTGTGGTTAGCTACACTC
TGAAGGACATTCACGATGACCAG...

(d) Clone 2: exon 3 spliced out

ATGTTTTTCACTTGTGGCCCAAATGAGGCCATGGTGGTCTCCGGATCTCTCTCAACACACTGACCCTCAA
TGTCAAGAGTGAAAAGGTTTACACTCGCCATGGGGTCCCCATCTCAGTCACTGGCATTGCCCAGGTAAAA
ATCCAGGGGCAGAACAAGGAGATGTTGGCGGCCGCCTGTCAGATGTTCCTGGGGAAGACGGAGGCTGAGA
TTGCCCACATTGCCCTGGAGACGTTAGAGGGCCACCAGAGGGCCATCATGGCCCACATGACTGTGGAGGA
GATCTATAAGGACAGGCAGAAATTCTCAGAACAGGTTTTCAAAGTGGCCTCCTCAGACCTGGTCAACATG
GGCATCAGTGTGGTTAGCTACACTCTGAAGGACATTCACGATGACCAG...

(e) Clone 7: deletion of 17 bp (#), exon 4 spliced out

ATGTTTTTCACTTGTGGCCCAAATGAGGCCATGGTGGTCTCCGGGTTCTGCCGAAGC############
####TGGAGGGCGTGTCTTTGTCCTGCCCTGCATCCAACAGATCCAGAGGTAAAAATCCAGGGGCAGAAC
AAGGAGATGTTGGCGGCCGCCTGTCAGATGTTCCTGGGGAAGACGGAGGCTGAGATTGCCCACATTGCCC
TGGAGACGTTAGAGGGCCACCAGAGGGCCATCATGGCCCACATGACTGTGGAGGAGATCTATAAGGACAG
GCAGAAATTCTCAGAACAGGTTTTCAAAGTGGCCTCCTCAGACCTGGTCAACATGGGCATCAGTGTGGTT
AGCTACACTCTGAAGGACATTCACGATGACCAG...

Figure III-12: Effects of F1 knock-out using CRISPR-Cas9 on mRNA level. Different exons are color-coded as follows: magenta: exon 2 beginning at the start codon; light blue: exon 3; blue-green: exon 4; green: exon 5; dark blue: exon 6. **(a)** WT human flotillin-1starting from ATG until exon 6; **(b)** F1-KO clone 2 with persisting insertion of A (highlighted in red) in exon 3 and precise loss of the whole exon 4; **(c)** F1-KO clone 2 without exons 3 – 5. Since the insertion of an A as a genomic mutation is located in exon 3, it is not detectable, as the complete exon 3 is missing; **(d)** F1-KO clone 2 with a precise loss of exon 3; **(e)** F1-KO clone 7 with a deletion of 17 bp in exon 3 (marked with #), as it was observed in the genomic DNA, but additional loss of exon 4. (Figure from Kapahnke, et al. 2016)

All mRNA transcript variants depicted in Figure III-12 result in a frameshift expected to be followed by a subsequent termination codon, which would cause a severely truncated protein product.

Figure III-13 shows the *in silico* translation of some of the observed mRNA variants. The mRNA variants of F1-KO clone 2 with a loss of exon 3 or 3 – 5, as shown in

Figure III-13b and c, result in an early stop codon after less than 20 residues from the N-terminus. In these cases, the protein product would be severely shortened and non-functional, so that the knock-out can be regarded as successful.

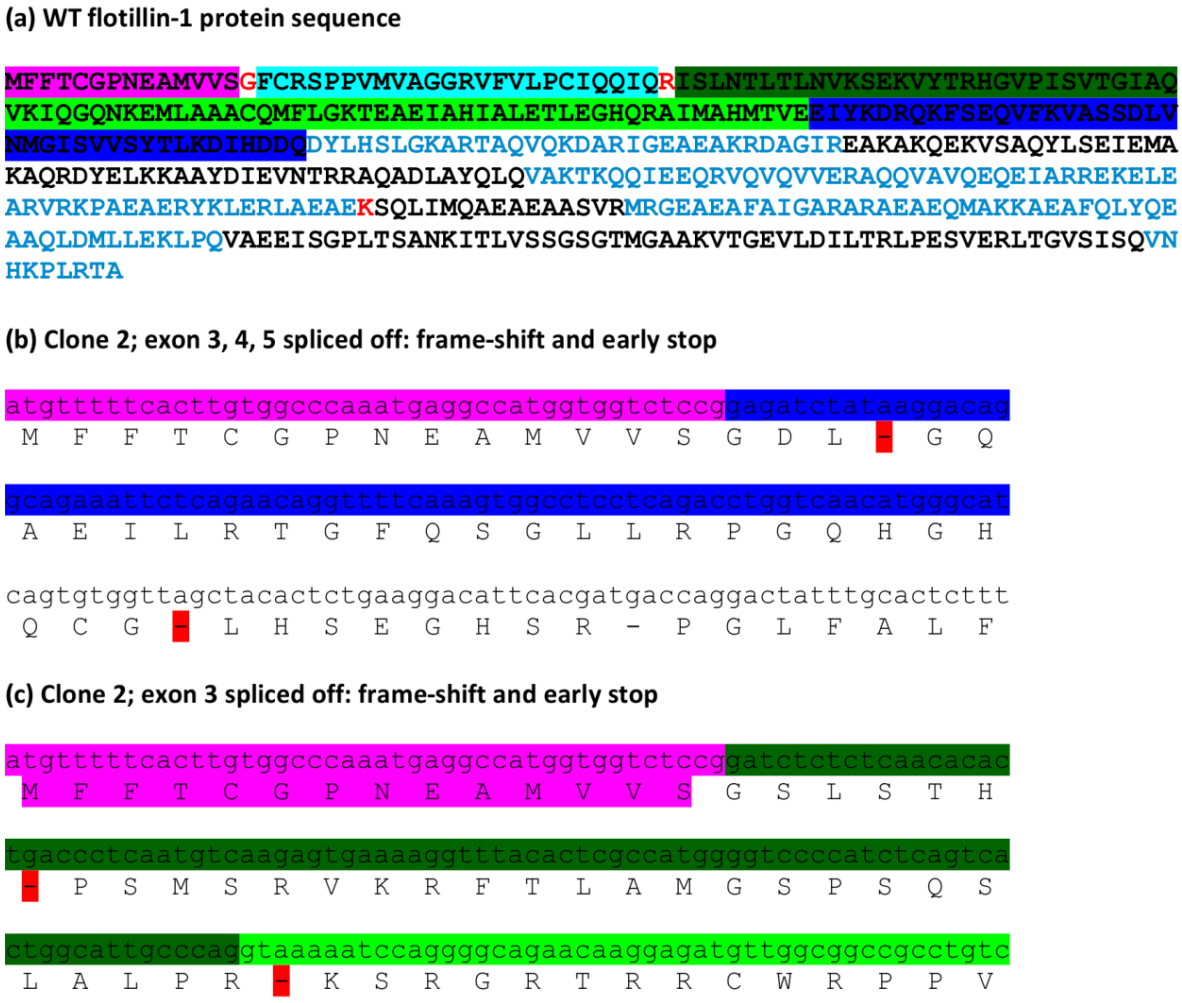

Figure III-13: *In silico* translation with the ExPASy Translate tool of mRNAs detected in the HeLa WT and several knock-out cell lines. Exon color-coding as in Figure III-12. **(a)** flotillin-1 WT protein sequence (in red: Amino acids compiled from flanking exons). **(b, c)** Amino acid sequences translated from mutant mRNA of F1-KO clone 2 resulted in a frameshift and thus an early stop codon (highlighted in red). (Figure from Kapahnke et al. 2016)

In contrast to this analysis, the translation of the cDNA variant of the F1-KO clone 2 shown in Figure III-12b, with persisting exon 3 (containing insertion of the extra A) but with a deletion of the whole exon 4, is able to produce a new protein. In the case of the mRNA seen in Figure III-12b, the resulting frameshift due to the insertion of A is corrected by the subsequent deletion of exon 4, which contains 91 bp. Thus, the correct reading frame beginning from exon 5 is recovered, since there is no stop codon in the frameshifted part until the end of exon 3. This results in a flotillin-1 protein product with 21 correct N-terminal amino acids, followed by 19 random amino acids, missing the amino acids coded by exon 4, but with correct protein sequence from exon 5 on (Figure III-14a). Also the mRNA variant of F1-KO clone 7 shown in Figure III-12e is expected to behave in a similar manner. Deletion of 17 bp and insertion of 1 bp, as seen in F1-KO clone 2, results in the same frameshift. The expected protein would consist of 19 N-terminal residues of flotillin-1, 15 random amino acids until the end of exon 3, followed by the flotillin-1 sequence starting with exon 5 (Figure III-14b).

This analysis shows that a frameshift caused by a double strand break on genomic DNA due to editing with CRISPR-Cas9 does not instantly result in the production of nonsense proteins. Some mRNA species may be translated into truncated proteins, whose functional impact cannot be predicted.

(a) F1-KO clone 2 mRNA: Insertion of an A in exon 3, exon 4 spliced out: first 21 residues from flotillin-1, followed by 19 random amino acids, recovery of correct flotillin-1 reading frame starting from residue 71 (=missing residues 22 – 70)

```
atgtttttcacttgtggcccaaatgaggccatggtggtctccggttctgccgaagcccc
 M   F   F   T   C   G   P   N   E   A   M   V   V   S   G   F   C   R   S   P

ccaagtcatggtggctggagggcgtgtctttgtcctgccctgcatccaacagatccagag
 P   S   H   G   G   W   R   A   C   L   C   P   A   L   H   P   T   D   P   E

gtaaaaatccaggggcagaacaaggagatgttggcggccgcctgtcagatgttcctgggg
 V   K   I   Q   G   Q   N   K   E   M   L   A   A   A   C   Q   M   F   L   G

aagacggaggctgagattgcccacattgccctggagacgttagagggccaccagagggcc
 K   T   E   A   E   I   A   H   I   A   L   E   T   L   E   G   H   Q   R   A

atcatggcccacatgactgtggaggagatctataaggacaggcagaaattctcagaacag
 I   M   A   H   M   T   V   E   E   I   Y   K   D   R   Q   K   F   S   E   Q
```

(b) F1-KO clone 7 mRNA: Deletion of 17 bp in exon 3, exon 4 spliced out: first 19 residues flotillin-1, then 15 random amino acids, recovery of correct flotillin-1 reading frame starting from residue 71 (=missing residues 20 – 70)

```
atgtttttcacttgtggcccaaatgaggccatggtggtctccggttctgccgaagctgg
 M   F   F   T   C   G   P   N   E   A   M   V   V   S   G   F   C   R   S   W

agggcgtgtctttgtcctgccctgcatccaacagatccagaggtaaaaatccaggggcag
 R   A   C   L   C   P   A   L   H   P   T   D   P   E   V   K   I   Q   G   Q

aacaaggagatgttggcggccgcctgtcagatgttcctggggaagacggaggctgagatt
 N   K   E   M   L   A   A   A   C   Q   M   F   L   G   K   T   E   A   E   I

gcccacattgccctggagacgttagagggccaccagagggccatcatggcccacatgact
 A   H   I   A   L   E   T   L   E   G   H   Q   R   A   I   M   A   H   M   T

gtggag...
 V   E...
```

Figure III-14: *In silico* translation of an mRNA species resulting in a frameshift and recovery of the correct reading frame due to the absence of exon 4, which contains 91 bp. Exons are colour-coded as described in Figure III-12. **(a)** F1-KO clone 2: The insertion of one A in exon 3, followed by removal of exon 4 is predicted to be translated into a truncated protein product that contains 21 regular flotillin-1 amino acids beginning from the N-terminus, followed by 19 random ones, and the correct flotillin-1 reading frame beginning again from residue 71. **(b)** F1-KO clone 7: The deletion of 17 bp results in the same frameshift as demonstrated in (a). The putative protein begins with 19 correct residues, followed by 15 random ones. Since exon 4 was removed, the reading frame is picked up correctly at residue 71, the beginning of exon 5. (Figure adapted from Kapahnke et al. 2016)

Assuming that the predicted translation, as illustrated in Figure III-14, is also taking place *in vivo*, the truncated proteins might be detectable by Western blot. To enhance the efficiency of detecting such aberrant proteins that might be unstable and easily degraded, protein degradation was inhibited with bafilomycin A (inhibitor of lysosomal acidification) or MG132 (proteasome inhibitor). In the F1-KO clone 2, no flotillin-1 protein fragments could be identified. However, in F1-KO clone 7, a band of about 44 kDa molecular mass, corresponding well to a calculated molecular mass of 43.5 kDa for the truncated protein described in Figure III-14b, could be detected (see Figure III-15). Furthermore, bands of a higher molecular mass than WT flotillin-1 were observed. These bands most likely represent the ubiquitinated proteins that remain undegraded upon proteasome-inhibiting conditions.

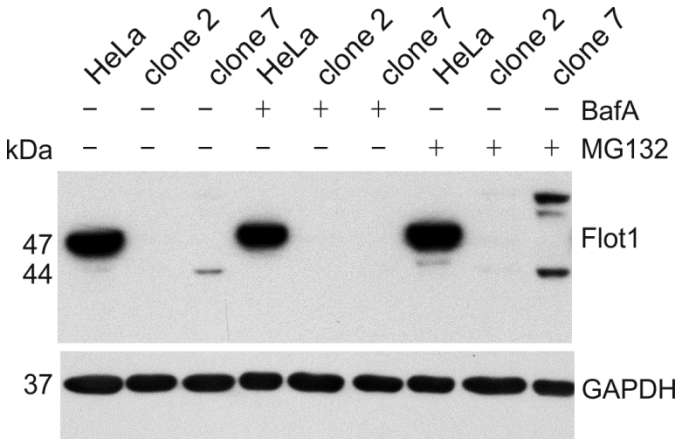

Figure III-15: Western blot analysis in untreated cells and in cells where the protein degradation was inhibited with 50 nM bafilomycin A (BafA) or 10 µM MG132 for 24 h. In F1-KO clone 7, treated with MG132, protein fragments can be detected at a molecular mass of 44 kDa and about 50 kDa. (Figure from Kapahnke et al. 2016)

IV. Discussion

IV.1 Accuracy of the CRISPR-Cas9 genome editing system

One of the most important concerns in genome editing by means of CRISPR-Cas9 is the occurrence of off-target effects due to not 100% precise DNA binding of the gRNAs. Off-target activity occurs on average in 50% of applications (Zhang et al. 2015). Hence, the development of more on-target specific Cas9 nucleases and the design of more gene-specific gRNAs has been the aim of many approaches to improve this novel technique. By now, there are several assays for off-target DSB detection available (Hu et al. 2016). Due to the improved gRNA design that reduces the appearance of off-target effects, the present study focused on the generation of KO cell lines, and no off-target detection assay was performed. Nevertheless, to enhance the reliability of the experiments with genome edited cells, off-target effects are frequently excluded by genome sequencing or sequencing of the most likely off-target loci. However, use of two or more single cell clones that contain different indel mutations in the target locus also improve the likelihood that those phenotypes arise from a specific change in the target locus.

The apparently simplest and most efficient approach to enhance the specificity of CRISPR-Cas9 is the design of a proper gRNA. There are numerous design engines freely available that result in a more specific targeting. In common, any validated gRNA sequence should differ in at least 2-3 nucleotides from any other sites in the target genome (Koo et al. 2015). gRNAs with two guanine nucleotides at their N-terminus provide a better on-target specificity (Cho et al. 2014). Paradoxically, using a truncated 17 nt long gRNA sequence can reduce off-target DNA cleavage in some cases. Due to their reduced binding energy to the DNA, such gRNA species are more sensitive to non-complementary binding and can more easily be removed from a binding site that is not 100% complementary. Unfortunately, such shorter binding sites that still differ at least 2-3 nt from any other sequence are much rarer in the human genome than 20 nt long ones (Fu et al. 2014). Thus, the gRNAs used for the experiments in this study were 20 nt long and were designed and cloned by the Horizon Discovery Group.

IV.2 Distribution pattern of flotillin family members in the knock-out cell lines

The subcellular localisation of flotillins can be variable and depends on the cell type and differentiation status of the cell. In HeLa cells, which were used in this study, flotillins reside predominantly at the plasma membrane (Banning et al. 2014). In immunofluorescence imaging of the generated F1 and F2 knock-out cell lines, the remaining flotillin (in case of F1-knock-out flotillin-2 and in case of F2 knock-out flotillin-1) was localised at the plasma membrane and, as expected, the double knock-out cells did not show any specific signal for flotillins.

Imaging experiments in other cell lines where flotillins have been found in multiple locations like plasma membrane and intracellular vesicles has so far been performed with knock-down cell lines (Banning et al. 2014). To validate the results of these studies and to exclude effects of persisting flotillins due to incomplete RNAi mediated knock-down, it might be useful to repeat such experiments with CRISPR-Cas9 mediated gene knock-out cell lines.

IV.3 Comparison to flotillin knock-down cells

Flotillins have been reported to be involved in growth factor signalling (Banning et al. 2014) as well as in apoptosis (John 2014). In growth factor signalling, flotillins have been shown to have different effects, with flotillin-1 knock-down resulting in a reduced activation of MAPK signalling (Amaddii et al. 2012) and flotillin-2 knock-down leading to a higher activation of MAPK signalling (Banning et al. 2014). Enhanced apoptosis of flotillin depleted cells has been described by John in her PhD thesis, and was interpreted as a consequence of survival signalling defects (John 2014).

The double-KO clone 1 was shown to have a significantly enhanced cleavage of PARP-1 upon treatment with staurosporin (see Figure III-4), indicating a higher rate of apoptosis. Similarly, in the second double-KO cell line under investigation, double-KO clone 2, there was a tendency to an augmentation of PARP-1 cleavage (see Figure III-4), but it was not significant. F1- and F2-single KOs did not show significant changes upon STS treatment. STS stimulation experiments were performed with an incubation time of 4 hours, but it is

possible that a more pronounced effect of STS could be detected at a longer incubation time. A time series study would be needed to obtain more precise data and to clarify the importance of flotillins in apoptosis.

Response of the knock-out cell lines generated in this study to EGF stimulation was not significantly different from wild-type HeLa cells (see Figure III-5). These results seem to stand in contrast to findings with transient flotillin knock-down in HeLa cells (Amaddii et al. 2012; Banning et al. 2014). This difference might be explained by the fact that experiments with transient knock-down HeLa cells were performed directly after flotillin depletion using RNAi. Hence, these cells did not have much time to adapt to the absence of flotillins. Experiments with flotillin-2 knock-out mice have shown that many cell-proliferative signalling pathways are upregulated, and the mice do not display any phenotypic changes as compared to the wild-type littermates (Banning et al. 2014). The upregulation of such compensatory pathways may have occurred also in flotillin knock-out HeLa cells, since experiments were performed weeks after genome editing procedure, and the cells thus had enough time to compensate for the loss of flotillins.

IV.4 Expression levels of flotillin mRNA in knock-out cells

RNAi mediated transcript knock-down is realised by a specific degradation of the target mRNA. In contrast to that, CRISPR-Cas9 causes a genomic mutation, followed by transcription of an incorrect mRNA that may be translated into a nonsense protein. Nevertheless, quantitative RT-PCR analysis showed a substantial reduction of 82% of flotillin mRNAs in some of the knock-out cell clones.

This reduction can possibly be explained by Nonsense-mediated mRNA Decay (NMD) (Popp and Maquat 2016). NMD is a cellular mechanism responsible for the degradation of mutated mRNAs with a premature stop codon. Hence, mRNAs containing a stop codon that is located more than 50 to 55 nt upstream of the last exon/intron border will be recognised and degraded by NMD.

Owing to this mechanism, it is strongly recommended to design high-quality sgRNA with a binding site preferably in an early exon (Popp and Maquat 2016). A resulting early indel mutation is expected to result in an early frameshift and thus an early premature stop

codon. As a consequence, the translated protein product would be highly truncated and most likely non-functioning. However, assuming that the remaining highly truncated protein still may retain a partial function, its production can be further reduced if premature stop codon is early enough to enable NMD. Therefore, the gRNAs for this study were designed to bind to exons 2 and 3 of the 13 exons (flotillin-1) and to exons 1 and 2 of the 11 exons (flotillin-2), so that these gRNAs were designed according to the state of the art.

IV.5 Indel mutations caused by CRISPR-Cas9 result in random splicing

Genome editing by means of CRISPR-Cas9 has emerged as a widely used tool in basic science, and there are already clinical trials using this approach in living human subjects as well (Sahel et al. 2019), bringing new ethical challenges to discuss. Knock-out using the CRISPR-Cas9 system introduces a DSB on genomic DNA that is predicted to be repaired by the error-prone NHEJ mechanism if there is no template available for HDR. If the resulting indel mutation is not a multiple of three, the reading frame gets changed, potentially resulting in a premature stop codon and thus in a highly truncated protein. This study shows that the consequences of genome editing with CRISPR-Cas9 are more far-reaching than the originally intended modification of a genomic DNA.

The high fidelity of the splicing machinery depends on many different factors, and the consequences of seemingly innocent genetic mutations on splicing are hard to predict (Baralle and Buratti 2017). In the present study, sequence analysis were not only performed with the genomic flotillin DNA, but also for the cDNA derived from flotillin mRNA. The results showed the expected indel mutation on genomic level. Surprisingly, also several flotillin mRNA variants were detected with larger segments of missing nucleotides that did not correspond to the respective genomic alterations. The missing segments, however, corresponded precisely to full exons. These mRNA variants that were observed in the same cell clone can only be explained by a loss of splicing fidelity due to the genomic indel mutation caused by CRISPR-Cas9, since alternative splicing has not yet been reported for flotillins.

This study was the first one reporting splicing errors in a human gene due to indel mutations after genome editing with CRISPR-Cas9. Previously, there have only been

studies showing altered splicing as a result of genomic variants in hereditary diseases. Mutations located in exon/intron borders result in exon skipping or intron retaining. Since gRNAs for knock-out cell lines obtained in this study were designed complementary to sequences in the middle of an exon, this effect was not observed. However, also mutations within an exon, as observed in this study, may lead to an impairment of splicing fidelity when they affect exonic splicing regulatory elements such a ESEs and ESSs (Teraoka et al. 1999).

Teraoka et al. analysed splicing consequences in different variants of mutations in the *ATM* gene of ataxia-telangiectasia patients. The underlying mutations were substitutions, deletions and insertions affecting only one, in a few cases also a number of bases. They reported different splicing variants in 48% of the mutated variants. In some cases, the splicing sites were created *de novo* by substitution of GC with GT or AA with AG, resulting in a truncated exon on the mature mRNA. The mutation of the recognition site GT to TT could lead to retention of the following intron in the mature mRNA (Teraoka et al. 1999).

Mutations of splicing regulators have emerged as a novel hallmark in cancer. The accurate splicing of exon 20 in the *HER2* gene is regulated by SRSF3 and hnRNPH1. Mutations of these regulators can be found in many breast cancers, leading to a truncated HER2 mRNA that lacks exon 20, with constitutive activation of the HER2 receptor and a low response to treatment with the monoclonal antibody Trastuzumab (Urbanski et al. 2018).

Our group has also shown that aberrant splicing after genome editing is not specific for flotillins or HeLa cells and also occurs in HEK 293T cells after CRISPR-Cas9 mediated knock-out of the *AGA* gene in exon 6. These data show that the aberrant splicing induced by gRNAs is neither flotillin nor cell line specific (Kapahnke et al. 2016).

In a later study, Mou et al. investigated the splicing effects in CRISPR-Cas9 edited *CTNNB1, KRAS* and *DMD* genes. Unexpectedly, they found a large deletion of 832 bp in the β-catenin gene in one cell clone, joining together the 3’ end of intron 2 to the 5’ end of exon 4. The skipping of exon 3 in the mRNA transcript consequently was not due to incorrect splicing, but rather the result of the genomic deletion of this exon (Mou et al. 2017). A mutation of such scale cannot be excluded in the cell clones investigated in this study, since primers for DNA sequencing in flotillin-1 enclose only a 576 bp long

fragment. Due to our analysis approach, it is possible that the number of the detected splicing variants and the genomic mutation variants in this study are not final, since only relatively few sequencing reactions were performed per clone. Increasing the number of sequenced samples it is likely to detect further splicing variants, as well as also more genomic alleles per cell clone, since HeLa cells are hypertriploid (Landry et al. 2013). For a complete analysis, high-throughput sequencing would be necessary, in a manner like it was performed by the group around Mou et al. (Mou et al. 2017).

Regarding the *in silico* translation of the mutated splicing variants, not all protein products were supposed to be highly truncated due to a premature stop codon. Figure III-14 shows a putative protein, with recovery of the correct reading frame, which might be functional or even act in a dominant negative fashion (Kapahnke et al. 2016). A band corresponding to the calculated molecular weight of this putative protein could be detected in a Western blot after proteasome inhibition with MG132 (Figure III-15). These results indicate that such a protein is expressed also *in vivo*, but is most likely highly unstable or dysfunctional, since the detection without inhibition of protein degradation was not successful. This instability might be the result of incapacity to associate with the plasma membrane, since palmitoylation at Cys34 (Morrow et al. 2002) and a hydrophobic domain from amino acid residue 1 to 36 (Liu et al. 2005) was shown to mediate the membrane association of flotillin-1. In the putative protein derived from the aberrant splicing variant, the frameshift begins at residue 22 (F1-KO clone 2) or 20 (F1-KO clone 7) (see Figure III-14) so that, first, the codon for Cys34 is shifted, resulting in the absence of this cysteine and subsequently also of the palmitoylation site and, second, a large part of the hydrophobic amino acid sequence is replaced by random amino acids from the beginning of the frameshift (see Figure IV-1). The correct reading frame is recovered at residue 71 (WT flotillin-1 as reference for numbering).

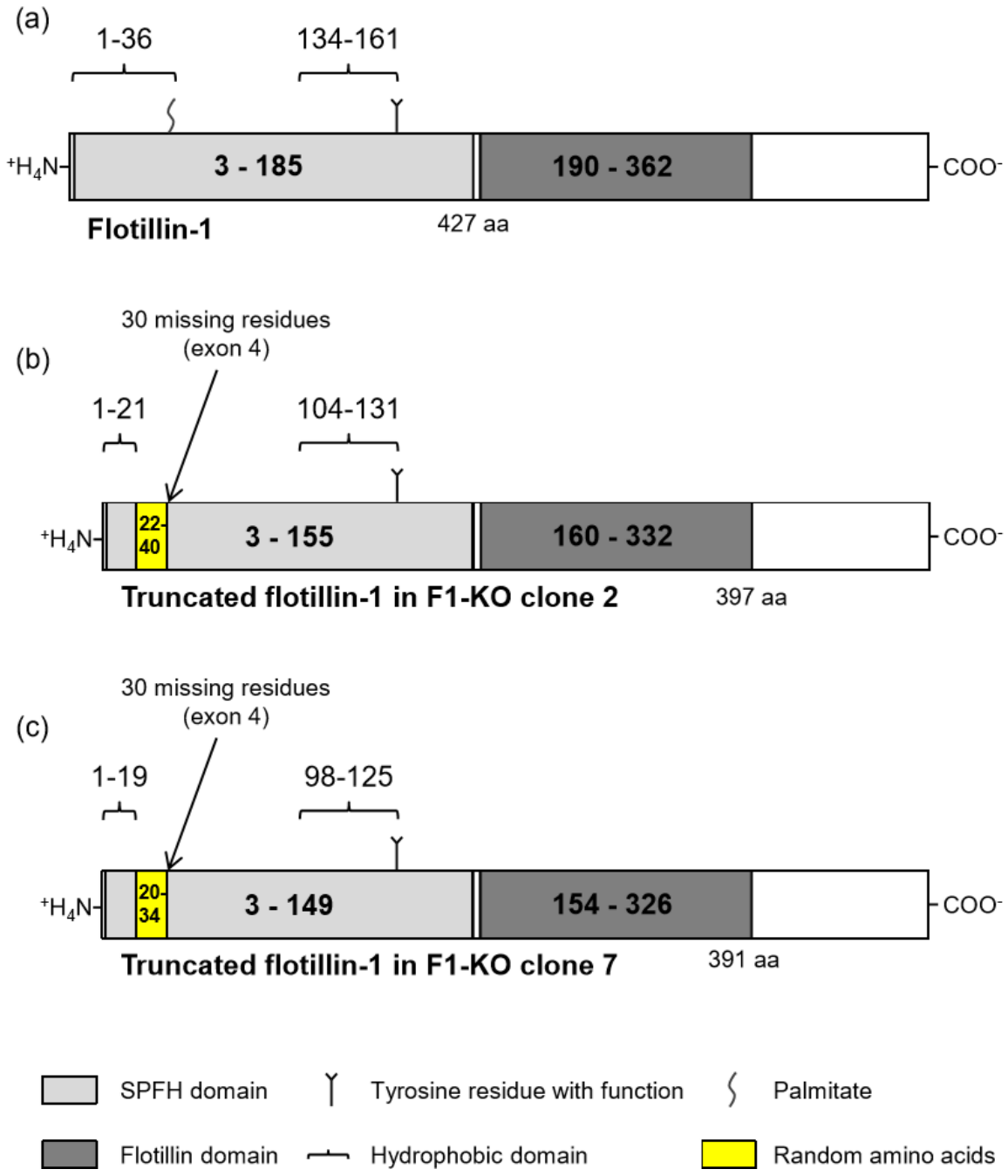

Figure IV-1: Predicted structure of aberrant flotillin-1 in the flotillin-1 knock-out cell clones F1-KO clone 2 and come 7. **(a)** Normal flotillin-1 has a hydrophobic domain spanning the first 36 amino acids and a palmitoylation motif at Cys34. These structures are a prerequisite for the correct membrane association of flotillin-1. **(b)** The indel mutation introduced by CRISPR-Cas9 leads to a frameshift and subsequent 21 random amino acids (yellow bar). The correct reading frame is recovered by the excision of the following exon 4 at residue 71 (WT flotillin-1 as reference for numbering). The random amino acid sequence is located in the first hydrophobic region, altering the second half of this region. A palmitoylated Cys at residue 34 in WT flotillin-1 is localised in this part as well, and is subsequently absent in the truncated protein. As a consequence, this mutated protein is predicted to be unable to stably associate with the plasma membrane. **(c)** A deletion of 17 bp in F1-KO clone 7 results in a similarly shifted reading frame as the insertion of one A. Thus, functional consequences are very similar, but numbering is different.

Mou et al. found a similar mRNA variant of β-catenin carrying a genomic mutation within exon 3 and resulting in an excision of the complete exon 3 (228 bp), which is a multiple of three bp exon. This mutated but functional protein was not immediately directed towards the degradation machinery, similarly to the truncated flotillin-1 in this study, enabling further analysis. Mou et al. found a different localisation pattern of this protein in immunofluorescence imaging, indicating a gain of function (Mou et al. 2017). Hence, the gene knock-out approach using CRISPR-Cas9 resulted in a complete opposite result from the original intention: A gain of function mutated protein. Regarding these data, great caution should be exercised in genome editing using CRISPR-Cas9. The control of knock-out success should not be monitored only by DNA sequencing, but also on mRNA and on protein level.

Aberrant splicing can obviously be a result of different genetic causes, since CRISPR-Cas9 mediated (Kapahnke et al. 2016), hereditary (Teraoka et al. 1999) as well as TALEN mediated (Lalonde et al. 2017) indel mutations have been reported to result in splicing errors. The exact mechanism how such indel mutations can cause erroneous splicing remains elusive. Further investigation is needed to be able to predict splicing effects of genome editing.

IV.6 Perspective of genome editing and gene therapy with CRISPR-Cas9

In the past years, CRISPR-Cas9 has emerged as a versatile tool for genome editing. Regarding the progress in enhanced on-target specificity, easier delivery methods and better detection rate of potential off-target effects, therapeutic use of this approach has become more and more an issue to discuss.

In our laboratory, CRISPR-Cas9 has become the approach of choice to generate knock-out cell lines. In most basic research projects, plasmid delivery is still the most common approach, as it is cost effective and easy to design (Sahel et al. 2019). The most sensitive step is to ensure an effective transfection rate, which often depends on the used cell line. By now, in our laboratory, flotillin-1, -2 and double-KOs have been generated in HeLa, HaCaT, HEK293T, hTERT, MCF7, U937 and COLO829 cells using electroporation, lipofection or lentiviral vectors for transfection. Using SpCas9-2A-Puro V2.2 as backbone

vector instead of pD1301-AD used for this study could facilitate the selection of knock-out cell clones due to a preselection based on a puromycin resistance.

In the past years, gene therapy has become a realistic perspective in the treatment of hereditary disorders, certain cancers or HIV (Sahel et al. 2019). Currently, there are clinical trials in phase 1 and phase 2 for sickle cell disease (NCT02186418) or HIV (NCT03164135) using CRISPR-Cas9 in a gene editing therapy. Even though off-target effects can be detected with more reliable techniques and new developments enhanced on-target specificity of CRISPR-Cas9, further effects of genome editing using this technique, such as aberrant splicing, cannot yet be predicted before the use in real patients. Thus, great caution should be taken using genome editing therapies in human subjects.

V. Summary

The CRISPR-Cas9 system has emerged as a versatile tool for genome editing. Using this novel technique, specific DNA modification can be achieved by designing a simple gRNA sequence complementary to the target site guiding the nuclease Cas9 towards it. The introduced double strand break is expected to be repaired by the error-prone non-homologous end joining repair, causing a frameshift leading to a premature stop codon and subsequently a highly truncated protein. In this study, the novel CRISPR-Cas9 approach was used to generate flotillin-1, flotillin-2 and double knock-out cell lines.

The screening of single cell clones was performed by Western blot and could detect several cell clones with absence of flotillin-1, flotillin-2 or both flotillin proteins. These cell clones were characterised in the following experiments. The real-time PCR showed a persistent presence of the flotillin mRNA, but a fundamental reduction in some cell clones, indicating degradation through NMD. EGF stimulation of the knock-out cell lines did not show significantly different results compared to HeLa wild-type, which can be interpreted as a consequence of adaptation to flotillin depleted conditions. The double-KO cell lines could be shown to react more sensitive to apoptosis induction upon staurosporin, but more precise results might be obtained in a time series study.

Sequence analysis of the genomic DNA and cDNA derived from mRNA showed the expected indel mutations on genomic DNA, but in addition to these mutations, several different mRNA variants were detected with apparently random missing exons. *In silico* translation of most mRNA variants resulted in a premature stop codon, but in two mRNA variants, a frameshift caused by a non-multiple of three indel mutation was corrected by excision of a subsequent exon containing the appropriate nucleotide number. The existence of the predicted protein was proven by Western blot after inhibition of protein degradation, upon which a band corresponding to the calculated molecular weight of the truncated protein was observed. Since this mutated protein could be detected only upon degradation inhibition, it is likely to be dysfunctional and unstable, but the functional consequences of such proteins cannot be predicted. In most studies using CRISPR-Cas9 for gene knock-out, the success is monitored only by sequencing of the genomic DNA. Regarding the results of this study, it is strongly recommended to verify the results also on mRNA and protein level.

VI. Zusammenfassung

In den letzten Jahren hat sich CRISPR-Cas9 zu einer vielseitig genutzten Methode in der Gentechnik entwickelt. Mit diesem Ansatz kann eine spezifische DNA-Modifikation erreicht werden, indem man eine einfache, zur Zielstelle komplementäre gRNA-Sequenz designt, welche die Nuklease Cas9 zur vorgesehenen Schnittstelle führt. Der so eingeführte Doppelstrangbruch wird nun durch die fehlerhafte *non-homologous end joining* Reparatur wieder zusammengefügt, was jedoch eine Leserasterverschiebung verursacht und zu einem vorzeitigen Stopcodon und damit zu einem stark verkürzten Protein führt. In dieser Arbeit wurde der neue CRISPR-Cas9-Ansatz verwendet, um Flotillin-1-, Flotillin-2- und Doppel-Knockout Zelllinien herzustellen.

Im Western Blot Screening der Einzelzellklone wurden mehrere Zellklone ohne Flotillin-1, Flotillin-2 oder ohne beide Flotillin-Proteinbanden nachgewiesen. Diese Zellklone wurden im Folgenden weiter charakterisiert. In der Real-time-PCR wurde weiterhin Flotillin-mRNA nachgewiesen, in einigen Zellklonen war diese jedoch stark verringert. Nach EGF-Stimulation konnte keine signifikant veränderte Signalantwort in Knockout-Zelllinien im Vergleich zum HeLa-Wildtyp beobachtet werden.

Die Sequenzierung genomischer DNA und aus mRNA hergestellter cDNA zeigte die erwarteten Indel-Mutationen auf genomischer DNA. Zusätzlich zu diesen Mutationen wurden jedoch mehrere unterschiedliche mRNA-Varianten mit scheinbar zufällig fehlenden Exons nachgewiesen. *In silico* Translation der meisten dieser mRNA-Varianten führte zu einem vorzeitigen Stopcodon. In zwei mRNA-Varianten jedoch wurde die durch die Indel-Mutationen verursachte Leserasterverschiebung durch das Ausschneiden eines nachfolgenden Exons mit der passenden Anzahl von Nukleotiden korrigiert. Dieses verkürzte Protein konnte nach Inhibierung des Proteinabbaus per Western Blot *in vivo* nachgewiesen werden, indem eine Bande detektiert wurde, die im Molekulargewicht mit der Berechnung für das verkürzte Protein übereinstimmte. Da dieses mutierte Protein nur nach Hemmung des Proteinabbaus nachgewiesen werden konnte, ist anzunehmen, dass es dysfunktional und instabil ist; dennoch können die funktionellen Konsequenzen solcher verkürzten Proteine nicht vorhergesagt werden. In vielen Anwendungsbereichen von CRISPR-Cas9 wird der Erfolg lediglich anhand von Sequenzierung genomischer DNA überprüft. Mit Blick auf die in dieser Arbeit erzielten Erkenntnisse sollte jedoch dringend empfohlen werden, Ergebnisse zusätzlich auf mRNA- und Proteinebene zu überprüfen.

VII. List of abbreviations

APS	Ammonium persulfate
BafA	Bafilomycin A
bp	Base pair
CIE	Clathrin-independent endocytosis
CRISPR	Clustered regulatory short palindromic repeats
crRNA	CRISPR-RNA
DSB	Double strand break
DEPC	Diethylpyrocarbonate
dk	Donkey
DMD	Dystrophin
DMEM	Dulbecco's modified eagle medium
DMSO	Dimethyl sulfoxide
dsRNA	Double strand RNA
ECL	Electrochemiluminescence
EDTA	Ethylenediaminetetraacetic acid
Egr1	Early growth response protein 1
ERK	Extracellular signal regulated kinase
ESE	Exonic splicing enhancer
ESS	Exonic splicing silencer
F1/2	Flotillin-1/-2
FCS	Fetal calf serum
GFP	Green Fluorescent Protein
gt	Goat
HDR	Homology directed repair
HER2	Human epidermal growth factor receptor 2
hnRNPH1	Heterogeneous nuclear ribonucleoprotein H
HRP	Horseradish peroxidase
ISE	Intronic splicing enhancer
ISS	Intronic splicing silencer
K-Ras	Kirsten rat sarcoma
LSM	Laser-Scanning-Microscope
MEK	MAPK/ERK Kinase
mRNA	Messenger RNA
ms	Mouse
NHEJ	Non-homologous end joining
NLS	Nuclear localisation sequence
NMD	Nonsense-mediated mRNA Decay

nt	Nucleotide
PBS	Phosphate buffered saline
PFA	Paraformaldehyde
PHB	Prohibitin homology
PI3K	Phosphoinositid-3-Kinase
RAF	Rapidly accelerating fibrosarcoma
RT-PCR	Real-time PCR
rb	Rabbit
RNAi	RNA interference
RNAP III	RNA-polymerase III
RNP	Ribonucleoprotein
SDS	Sodium dodecyl sulfate
siRNA	Short interfering RNA
snRNP	Small nuclear ribonucleoprotein particle
SPFH	Stomatin, prohibitin, flotillin and HflC and K
SRSF3	Serine and arginine rich splicing Factor 3
STS	Staurosporin
TEMED	Tetramethylethylenediamine
tif	Tagged Image File Format
tracrRNA	Trans-activating-CRISPR-RNA
WT	Wild-type

VIII. List of figures

IX. List of tables

X. References

Amaddii, M., M. Meister, A. Banning, A. Tomasovic, J. Mooz, K. Rajalingam, and R. Tikkanen. 2012. 'Flotillin-1/Reggie-2 Protein Plays Dual Role in Activation of Receptor-Tyrosine Kinase/Mitogen-Activated Protein Kinase Signaling'. *Journal of Biological Chemistry* 287(10): 7265–78.

Babuke, T., M. Ruonala, M. Meister, M. Amaddii, C. Genzler, A. Esposito, and R. Tikkanen. 2009. 'Hetero-Oligomerization of Reggie-1/Flotillin-2 and Reggie-2/Flotillin-1 Is Required for Their Endocytosis'. *Cellular Signalling* 21(8): 1287–97.

Banning, A., W. Ockenga, F. Finger, P. Siebrasse, and R. Tikkanen. 2012. 'Transcriptional Regulation of Flotillins by the Extracellularly Regulated Kinases and Retinoid X Receptor Complexes'. *PLoS ONE* 7(9).

Banning, A., N. Kurrle, M. Meister, and R. Tikkanen. 2014. 'Flotillins in Receptor Tyrosine Kinase Signaling and Cancer.' *Cells* 3(1): 129–49.

Banning, A., C. Regenbrecht, and R. Tikkanen. 2014. 'Increased Activity of Mitogen Activated Protein Kinase Pathway in Flotillin-2 Knockout Mouse Model'. *Cellular Signalling* 26(2): 198–207.

Baralle, D., and E. Buratti. 2017. 'RNA Splicing in Human Disease and in the Clinic'. *Clinical Science* 131(5): 355–68.

Baumann, C., V. Ribon, M. Kanzaki, D. Thurmond, S. Mora, S. Shigematsu, P. Bickel, J. Pessin, and A. Saltiel. 2000. 'CAP Defines a Second Signalling Pathway Required for Insulin-Stimulated Glucose Transport'. *Nature* 407(6801): 202–7.

Bickel, P., P. Scherer, J. Schnitzer, P. Oh, M. Lisanti, and H. Lodish. 1997. 'Flotillin and Epidermal Surface Antigen Define a New Family of Caveolae-Associated Integral Membrane Proteins.' *The Journal of biological chemistry* 272(21): 13793–802.

Brody, E., and J. Abelson. 1985. 'The "Spliceosome": Yeast Pre-Messenger RNA Associates with a 40S Complex in a Splicing-Dependent Reaction'. *Science* 228(4702): 963–67.

Browman, D., M. Hoegg, and S. Robbins. 2007. 'The SPFH Domain-Containing Proteins: More than Lipid Raft Markers'. *Trends in Cell Biology* 17(8): 394–402.

Buratti, E., and F. Baralle. 2004. 'Influence of RNA Secondary Structure on the Pre-MRNA Splicing Process.' *Molecular and cellular biology* 24(24): 10505–14.

Cáceres, J., and A. Kornblihtt. 2002. 'Alternative Splicing: Multiple Control Mechanisms and Involvement in Human Disease'. *Trends in Genetics* 18(4): 186–93.

Cho, S., S. Kim, Y. Kim, J. Kweon, H. Kim, S. Bae, and J. Kim. 2014. 'Analysis of Off-Target Effects of CRISPR/Cas-Derived RNA-Guided Endonucleases and Nickases'. *Genome Research* 24(1): 132–41.

Ding, Q., Y. Lee, E. Schaefer, D. Peters, A. Veres, K. Kim, N. Kuperwasser, D. Motola, T. Meissner, W. Hendriks, M. Trevisan, R. Gupta, A. Moisan, E. Banks, M. Friesen, R. T. Schinzel, F. Xia, A. Tang, Y. Xia, E. Figueroa, A. Wann, T. Ahfeldt, L. Daheron, F. Zhang, L. Rubin, L. Peng, R. Chung, K. Musunuru, and C. Cowan. 2013. 'A TALEN Genome-Editing System for Generating Human Stem Cell-Based Disease Models'. *Cell Stem Cell* 12(2): 238–51.

Frick, M., N. Bright, K. Riento, A. Bray, C. Merrified, and B. Nichols. 2007. 'Coassembly of Flotillins Induces Formation of Membrane Microdomains, Membrane Curvature, and Vesicle Budding'. *Current Biology* 17(13): 1151–56.

Fu, Y., J. Foden, C. Khayter, M. Maeder, D. Reyon, J. Joung, and J. Sander. 2013. 'High-Frequency off-Target Mutagenesis Induced by CRISPR-Cas Nucleases in Human Cells'. *Nature Biotechnology* 31(9): 822–26.

Fu, Y., J. Sander, D. Reyon, V. Cascio, and J. Joung. 2014. 'Improving CRISPR-Cas Nuclease Specificity Using Truncated Guide RNAs'. *Nature Biotechnology* 32(3): 279–84.

Glebov, O., N. Bright, and B. Nichols. 2006. 'Flotillin-1 Defines a Clathrin-Independent Endocytic Pathway in Mammalian Cells'. *Nature Cell Biology* 8(1): 46–54.

Hesselberth, J. 2013. 'Lives That Introns Lead after Splicing'. *Wiley Interdisciplinary Reviews: RNA* 4(6): 677–91.

Horvath, P., and R. Barrangou. 2010. 'CRISPR/Cas, the Immune System of Bacteria and Archaea'. *Science* 327(5962): 167–70.

Hu, J., M. Meyers, J. Dong, R. Panchakshari, F. Alt, and R. Frock. 2016. 'Detecting DNA Double-Stranded Breaks in Mammalian Genomes by Linear Amplification-Mediated High-Throughput Genome-Wide Translocation Sequencing'. *Nature Protocols* 11(5): 853–71.

Iannone, C., and J. Valcárcel. 2013. 'Chromatin's Thread to Alternative Splicing Regulation'. *Chromosoma* 122(6): 465–74.

Jacobi, A., G. Rettig, R. Turk, M. Collingwood, S. Zeiner, R. Quadros, D. Harms, P. Bonthuis, C. Gregg, M. Ohtsuka, C. Gurumurthy, and M. Behlke. 2017. 'Simplified CRISPR Tools for Efficient Genome Editing and Streamlined Protocols for Their Delivery into Mammalian Cells and Mouse Zygotes.' *Methods* 121–122: 16–28.

John, B. 2014. 'Function of Flotillins in Alzheimer' s Disease and Apoptosis'. *PhD Thesis, Johann-Wolfgang-Goethe-University, Frankfurt am Main*.

John, B., M. Meister, A. Banning, and R. Tikkanen. 2014. 'Flotillins Bind to the Dileucine Sorting Motif of β-Site Amyloid Precursor Protein-Cleaving Enzyme 1 and Influence Its Endosomal Sorting'. *FEBS Journal* 281(8): 2074–87.

Kapahnke, M., A. Banning, and R. Tikkanen. 2016. 'Random Splicing of Several Exons Caused by a Single Base Change in the Target Exon of CRISPR/Cas9 Mediated Gene Knockout'. *Cells* 5(4): 45.

Khanna, A., and S. Stamm. 2010. 'Regulation of Alternative Splicing by Short Non-Coding Nuclear RNAs.' *RNA biology* 7(4): 480–85.

Kim, Y., J. Cha, and S. Chandrasegaran. 1996. 'Hybrid Restriction Enzymes: Zinc Finger Fusions to Fok I Cleavage Domain'. *Proceedings of the National Academy of Sciences of the United States of America* 93(3): 1156–60.

Koo, T., J. Lee, and J. Kim. 2015. 'Measuring and Reducing Off-Target Activities of Programmable Nucleases Including CRISPR-Cas9.' *Molecules and cells* 38(6): 475–81.

Kurrle, N., F. Völlner, R. Eming, M. Hertl, A. Banning, and R. Tikkanen. 2013. 'Flotillins Directly Interact with γ-Catenin and Regulate Epithelial Cell-Cell Adhesion.' *PloS one* 8(12): e84393.

Kurrle, N., W. Ockenga, M. Meister, F. Völlner, S. Kühne, B. John, A. Banning, and R. Tikkanen. 2013. 'Phosphatidylinositol 3-Kinase Dependent Upregulation of the Epidermal Growth Factor Receptor upon Flotillin-1 Depletion in Breast Cancer Cells'. *BMC Cancer* 13.

Lalonde, S., O. Stone, S. Lessard, A. Lavertu, J. Desjardins, M. Beaudoin, M. Rivas, D. Stainier, and G. Lettre. 2017. 'Frameshift Indels Introduced by Genome Editing Can Lead to In-Frame Exon Skipping'. *PLoS ONE* 12(6).

Landry, J., P. Pyl, T. Rausch, T. Zichner, M. Tekkedil, A. Stütz, A. Jauch, R. Aiyar, G. Pau, N. Delhomme, J. Gagneur, J. Korbel, W. Huber, and L. Steinmetz. 2013. 'The Genomic and Transcriptomic Landscape of a Hela Cell Line'. *G3: Genes, Genomes, Genetics* 3(8): 1213–24.

Liu, J., S. DeYoung, M. Zhang, L. Dold, and A. Saltiel. 2005. 'The Stomatin/Prohibitin/Flotillin/HflK/C Domain of Flotillin-1 Contains Distinct Sequences That Direct Plasma Membrane Localization and Protein Interactions in 3T3-L1 Adipocytes'. *Journal of Biological Chemistry* 280(16): 16125–34.

Makarova, K., D. Haft, R. Barrangou, S. Brouns, P. Horvath, S. Moineau, F. Mojica, Y. Wolf, A. Yakunin, J. Van Der Oost, and E. Koonin. 2011. 'Evolution and Classification of the CRISPR-Cas Systems'. *Nat Rev Microbiol* 9(6): 467–77.

Mali, P., K. Esvelt, and G. Church. 2013. 'Cas9 as a Versatile Tool for Engineering Biology'. *Nature Methods* 10(10): 957–63.

Meister, M. 2014. 'A Novel Role for Flotillins in Activation and Endosomal Sorting of Transmembrane Receptors.' *PhD Thesis, Johann-Wolfgang-Goethe-University, Frankfurt am Main*.

Meister, M,, and R. Tikkanen. 2014. 'Endocytic Trafficking of Membrane-Bound Cargo: A Flotillin Point of View'. *Membranes* 4(3): 356–71.

Morrow, I., S. Rea, S. Martin, I. Prior, R. Prohaska, J. Hancock, D. James, and R. Parton. 2002. 'Flotillin-1/Reggie-2 Traffics to Surface Raft Domains via a Novel Golgi-Independent Pathway. Identification of a Novel Membrane Targeting Domain and a Role for Palmitoylation'. *Journal of Biological Chemistry* 277(50): 48834–41.

Morrow, I., and R. Parton. 2005. 'Flotillins and the PHB Domain Protein Family: Rafts Worms and Anaesthetics'. *Traffic* 6(9): 725–40.

Mou, H., J. Smith, L. Peng, H. Yin, J. Moore, X. Zhang, C. Song, A. Sheel, Q. Wu, D. Ozata, Y. Li, D. Anderson, C. Emerson, E. Sontheimer, M. Moore, Z. Weng, and W. Xue. 2017. 'CRISPR/Cas9-Mediated Genome Editing Induces Exon Skipping by Alternative Splicing or Exon Deletion.' *Genome biology* 18(1): 108.

Neumann-Giesen, C., B. Falkenbach, P. Beicht, S. Claasen, G. Lüers, C. Stuermer, V. Herzog, and R. Tikkanen. 2004. 'Membrane and Raft Association of Reggie-1/Flotillin-2: Role of Myristoylation, Palmitoylation and Oligomerization and Induction of Filopodia by Overexpression'. *Biochemical Journal* 378(2): 509–18.

Neumann-Giesen, C., I. Fernow, M. Amaddii, and R. Tikkanen. 2007. 'Role of EGF-Induced Tyrosine Phosphorylation of Reggie-1/Flotillin-2 in Cell Spreading and Signaling to the Actin Cytoskeleton'. *Journal of Cell Science* 120(3): 395–406.

Newman, A. 1998. 'RNA Splicing'. *Current Biology* 8(25): 903–5.

Popp, M., and L. Maquat. 2016. 'Leveraging Rules of Nonsense-Mediated MRNA Decay for Genome Engineering and Personalized Medicine'. *Cell* 165(6): 1319–22.

Ran, F., P. Hsu, J. Wright, V. Agarwala, D. Scott, F. Zhang. 2013. 'Genome Engineering Using the CRISPR-Cas9 System HHS Public Access Author Manuscript'. *Nat Protoc* 8(11): 2281–2308.

Rana, T. 2007. 'Illuminating the Silence: Understanding the Structure and Function of Small RNAs'. *Nature Reviews Molecular Cell Biology* 8(1): 23–36.

Resnik, N., K. Sepcic, A. Plemenitas, R. Windoffer, R. Leube, and P. Veranic. 2011. 'Desmosome Assembly and Cell-Cell Adhesion Are Membrane Raft-Dependent Processes.' *The Journal of biological chemistry* 286(2): 1499–1507.

Sahel, D., A. Mittal, and D. Chitkara. 2019. 'CRISPR/Cas System for Genome Editing: Progress and Prospects as a Therapeutic Tool'. *Journal of Pharmacology and Experimental Therapeutics* 370(3): 725–35.

Schroeder, W., S. Stewart-Galetka, S. Mandavilli, D. Parry, L. Goldsmith, and M. Duvic. 1994. 'Cloning and Characterization of a Novel Epidermal Cell Surface Antigen (ESA)'. *Journal of Biological Chemistry* 269(31): 19983–91.

Schulte, T., K. Paschke, U. Laessing, F. Lottspeich, and C. Stuermer. 1997. 'Reggie-1 and Reggie-2, Two Cell Surface Proteins Expressed by Retinal Ganglion Cells during Axon Regeneration.' *Development (Cambridge, England)* 124(2): 577–87.

Shin, C., and J. Manley. 2004. 'Cell Signalling and the Control of Pre-MRNA Splicing.' *Nature reviews. Molecular cell biology* 5(9): 727–38.

Simons, K., and M. Gerl. 2010. 'Revitalizing Membrane Rafts: New Tools and Insights'. *Nature Reviews Molecular Cell Biology* 11(10): 688–99.

Solis, G., M. Hoegg, C. Munderloh, Y. Schrock, E. Malaga-Trillo, E. Rivera-Milla, and C. Stuermer. 2007. 'Reggie/Flotillin Proteins Are Organized into Stable Tetramers in Membrane Microdomains'. *Biochemical Journal* 403(2): 313–22.

Sorkina, Tatiana, John Caltagarone, and Alexander Sorkin. 2013. 'Flotillins Regulate Membrane Mobility of the Dopamine Transporter but Are Not Required for Its Protein Kinase C Dependent Endocytosis'. *Traffic* 14(6): 709–24.

Staley, J., and C. Guthrie. 1998. ‘Mechanical Devices of the Spliceosome: Motors, Clocks, Springs, and Things’. *Cell* 92(3): 315–26.

Stuermer, C., D. Lang, F. Kirsch, M. Wiechers, S. Deininger and H. Plattner. 2001. ‘Glycosylphosphatidyl Inositol-anchored Proteins and fyn Kinase Assemble in Noncaveolar Plasma Membrane Microdomains Defined by Reggie-1 and -2’. *Molecular Biology of the Cell* 12: 3031–45.

Teraoka, N., M. Telatar, S. Becker-Catania, T. Liang, S. Önengüt, A. Tolun, L. Chessa, Ö. Sanal, E. Bernatowska, R. Gatti, and P. Concannon. 1999. ‘Splicing Defects the Ataxia-Telangiectasia Gene, ATM: Underlying Mutations and Consequences’. *American Journal of Human Genetics* 64(6): 1617–31.

Urbanski, L., N. Leclair, and O. Anczuków. 2018. ‘Alternative-Splicing Defects in Cancer: Splicing Regulators and Their Downstream Targets, Guiding the Way to Novel Cancer Therapeutics’. *Wiley Interdisciplinary Reviews: RNA* 9(4): 1–36.

Vakulskas, C., D. Dever, G. Rettig, R. Turk, A. Jacobi, M. Collingwood, N. Bode, M. McNeill, S. Yan, J. Camarena, C. Lee, S. Park, V. Wiebking, R. Bak, N. Gomez-Ospina, M. Pavel-Dinu, W. Sun, G. Bao, M. Porteus, and M. Behlke. 2018. ‘A High-Fidelity Cas9 Mutant Delivered as a Ribonucleoprotein Complex Enables Efficient Gene Editing in Human Hematopoietic Stem and Progenitor Cells’. *Nature Medicine* 24(8): 1216–24.

Vakulskas, C., and M. Behlke. 2019. ‘Evaluation and Reduction of CRISPR Off-Target Cleavage Events’. *Nucleic Acid Therapeutics* 29(4): 167–74.

Vockley, J., P. Rogan, B. Anderson, J. Willard, R. Seelan, D. Smith, and W. Liu. 2000. ‘Exon Skipping in IVD RNA Processing in Isovaleric Acidemia Caused by Point Mutations in the Coding Region of the IVD Gene’. *American Journal of Human Genetics* 66(2): 356–67.

Völlner, F., J. Ali, N. Kurrle, Y. Exner, R. Eming, M. Hertl, A. Banning, and R. Tikkanen. 2016. ‘Loss of Flotillin Expression Results in Weakened Desmosomal Adhesion and Pemphigus Vulgaris-like Localisation of Desmoglein-3 in Human Keratinocytes’. *Scientific Reports* 6.

Wang, G., and T. Cooper. 2007. ‘Splicing in Disease: Disruption of the Splicing Code and the Decoding Machinery’. *Nature Reviews Genetics* 8(10): 749–61.

Wang, J., X. Zhang, L. Cheng, and Y. Luo. 2019. ‘An Overview and Metanalysis of Machine and Deep Learning-Based CRISPR gRNA Design Tools’. *RNA Biology* 17(1): 1–10.

Zaharieva, E., J. Chipman, and M. Soller. 2012. ‘Alternative Splicing Interference by Xenobiotics.’ *Toxicology* 296(1–3): 1–12.

Zhang, X., L. Tee, X. Wang, Q. Huang, and S. Yang. 2015. ‘Off-Target Effects in CRISPR/Cas9-Mediated Genome Engineering.’ *Molecular therapy. Nucleic acids* 4(e264): 1–8 .

XI. List of publications

Kapahnke M, Banning A, Tikkanen R. Random Splicing of Several Exons Caused by a Single Base Change in the Target Exon of CRISPR/Cas9 Mediated Gene Knockout. *Cells*. 2016;5(4):45. doi:10.3390/cells5040045. (IF 5.656)

Citations on PubMed: 17 (https://www.mdpi.com/2073-4409/5/4/45 - 06/11/2020)

XII. Declaration

„Hiermit erkläre ich, dass ich die vorliegende Arbeit selbständig und ohne unzulässige Hilfe oder Benutzung anderer als der angegebenen Hilfsmittel angefertigt habe. Alle Textstellen, die wörtlich oder sinngemäß aus veröffentlichten oder nichtveröffentlichten Schriften entnommen sind, und alle Angaben, die auf mündlichen Auskünften beruhen, sind als solche kenntlich gemacht. Bei den von mir durchgeführten und in der Dissertation erwähnten Untersuchungen habe ich die Grundsätze guter wissenschaftlicher Praxis, wie sie in der „Satzung der Justus-Liebig-Universität Gießen zur Sicherung guter wissenschaftlicher Praxis“ niedergelegt sind, eingehalten sowie ethische, datenschutzrechtliche und tierschutzrechtliche Grundsätze befolgt. Ich versichere, dass Dritte von mir weder unmittelbar noch mittelbar geldwerte Leistungen für Arbeiten erhalten haben, die im Zusammenhang mit dem Inhalt der vorgelegten Dissertation stehen, oder habe diese nachstehend spezifiziert. Die vorgelegte Arbeit wurde weder im Inland noch im Ausland in gleicher oder ähnlicher Form einer anderen Prüfungsbehörde zum Zweck einer Promotion oder eines anderen Prüfungsverfahrens vorgelegt. Alles aus anderen Quellen und von anderen Personen übernommene Material, das in der Arbeit verwendet wurde oder auf das direkt Bezug genommen wird, wurde als solches kenntlich gemacht. Insbesondere wurden alle Personen genannt, die direkt und indirekt an der Entstehung der vorliegenden Arbeit beteiligt waren. Mit der Überprüfung meiner Arbeit durch eine Plagiatserkennungssoftware bzw. ein internetbasiertes Softwareprogramm erkläre ich mich einverstanden.“

Gießen 09/11/2020 Marcel Kapahnke

XIII. Acknowledgements

Ich danke herzlich allen Menschen, die mir im Verlauf meines Studiums und meiner Promotion zur Seite standen. Ohne Euch alle wäre es mir nicht möglich gewesen, diese Promotionsarbeit anzufertigen.

Mein aufrichtigster Dank gilt meiner Doktormutter Frau Prof. Dr. Ritva Tikkanen dafür, dass sie mir die Möglichkeit gegeben hat, diese Doktorarbeit hier in Ihrer Arbeitsgruppe anzufertigen und für all die praktische Unterstützung im Labor sowie auch für die anregenden Diskussionen zum Thema dieser Arbeit. Außerdem danke ich herzlichst meiner Betreuerin Frau Dr. Antje Banning für die alltägliche Anleitung und die gute Betreuung in allen Bereichen. Petra Janson und Ralf Füllkrug möchte ich für ihre große Hilfsbereitschaft und die belebte Zusammenarbeit im Labor danken. Von der gesamten Arbeitsgruppe fühlte ich mich stets herzlich aufgenommen und werde mich immer mit Freude an die gemeinsame Zeit mit Euch zurück erinnern. Bei Herrn Prof. Dr. Wolfgang Kummer bedanke ich mich sehr für die Bereitstellung der Förderung dieses Projekts durch die Landes-Offensive zur Entwicklung wissenschaftlich-ökonomischer Exzellenz (LOEWE).

Meiner gesamten Familie möchte ich danken für den großen Zusammenhalt, den wir haben, und dafür, dass Ihr mich immer gerne unterstützt. Ich bin unglaublich froh, mich so sehr liebende Eltern und einen Bruder zu haben, die mich schon seit meiner Kindheit begleiten und an die ich mich in allen Lebenssituationen wenden kann wohl wissend, dass sie immer für mich da sind. Liebe Mama, ich danke Dir dafür, dass ich mich in allen Lebenslagen vertrauensvoll an Dich wenden kann und ich zweifellos auf Deine Unterstützung zählen kann. Ich weiß ganz sicher, dass Du, mein lieber Papa, mir gerne sachkundig als promovierter Chemiker genauso aber auch persönlich als mein Vater während der gesamten Zeit meines Studiums Deinen Rat gegeben hättest. Lieber Pascal, mein Bruderherz, ich weiß, dass ich in allen Situationen im Leben immer auf Dich bauen kann und freue mich auf alle Unternehmungen, die wir noch gemeinsam vorhaben.

Mi sento davvero fortunato ad avere una fidanzata così speciale e affettuosa come te cara Giulia. Ti ringrazio per starmi vicino in tutte le situazioni e per darmi forza e fiducia nei momenti più difficili. Nonostante tutte le distanze riusciamo sempre a ritrovarci. Sei la persona che completa ogni parte della mia vita.

Liebe Freunde aus der Heimat, dem Studium oder anderen Lebensphasen, Euch kennen gelernt zu haben hat mein Leben bereichert. Ich danke Euch allen für die schöne Zeit zusammen und dafür, dass Ihr mich so oft unterstützt.